Universidade de Aveiro
2021

Daniel Girão Monteiro

Unravelling the profile and role of tRNA-derived small RNAs in Influenza A virus infection

Estudo do perfil e função de pequenos fragmentos de RNA derivados de tRNA durante a infeção pelo vírus da Influenza A

2021

Universidade de Aveiro
2021

Daniel Girão Monteiro

Unravelling the profile and role of tRNA-derived small RNAs in Influenza A virus infection

Estudo do perfil e função de pequenos fragmentos de RNA derivados de tRNA durante a infeção pelo vírus da Influenza A

Dissertação apresentada à Universidade de Aveiro para cumprimento dos requisitos necessários à obtenção do grau de Mestre em Microbiologia, realizada sob a orientação científica da Doutora Daniela Ribeiro, Investigadora Auxiliar do Departamento de Ciências Médicas e Investigadora Principal do "Virus Host-Cell Interactions Laboratory" do Instituto de Biomedicina (iBiMED), Departamento de Ciências Médicas, Universidade de Aveiro e da Doutora Ana Raquel Soares, Investigadora Auxiliar do Departamento de Ciências Médicas e do Instituto de Biomedicina (iBiMED) da Universidade de Aveiro

This work was supported by the Portuguese Foundation for Science and Technology (FCT): PTDC/BIACEL/31378/2017 (POCI-01-0145-FEDER-031378), POCI01-0145-FEDER-029843, CEECIND/03747/2017, CEECIND/00284/2018 UID/BIM/04501/2013, POCI-01-0145-FEDER-007628 under the scope of the Operational Program "Competitiveness and internationalization", in its FEDER/FNR component.

It was also supported by the European Union thought the Horizon 2020 program: H2020-WIDESPREAD-2020-5 ID-952373.

Image acquisition was performed in the LiM facility of iBiMED, a node of PPBI (Portuguese Platform of BioImaging): POCI-01-0145-FEDER-022122.

o júri

presidente	Prof. Doutora Sónia Alexandra Leite Velho Mendo Barroso Professora Auxiliar c/ Agregação, Departamento de Biologia, Universidade de Aveiro
Vogal – Arguente	Doutora Mafalda Raquel da Conceição Santos Investigadora Doutorada (nível 1), i3S – Instituto de Investigação e Inovação em Saúde, Universidade do Porto
Vogal – Orientadora	Doutora Daniela Maria Oliveira Gandra Ribeiro Equiparada a Investigadora Auxiliar, Departamento de Ciências Médicas, Universidade de Aveiro

agradecimentos

Em primeiro lugar, quero agradecer à Dr. Daniela Ribeiro e à Dr. Ana Raquel Soares por toda a orientação, acompanhamento e conhecimento que me transmitiram nesta difícil etapa. Quero agradecer também por me terem aberto as portas ao mundo da investigação nos campos da virologia e dos RNAs, duas áreas que sempre me fascinaram e em que sempre quis trabalhar.

Quero agradecer ao grupo fantástico que partilhou o laboratório comigo e ao longo destes meses me ajudou, mostrando toda a disponibilidade e paciência para as minhas dúvidas e problemas e me mostraram o que é verdadeiramente fazer parte de um laboratório científico.

Um obrigado muito especial a toda a minha família e amigos, por tudo o que fizeram e fazem por mim, especialmente aos meus pais, por todo o esforço durante todos estes anos, principalmente nestes dois últimos em que saí de casa e me mudei para Aveiro, com todas as viagens semanais.

Um grande obrigado à Gabriela por ter estado sempre disponível para me ouvir, principalmente nos momentos mais complicados e stressantes, em que me deu ânimo, motivação e calma para ultrapassar estes momentos menos bons.

Por fim, quero deixar uma palavra de agradecimento a todos os membros da Residência Lourenço Peixinho. Obrigado por terem tornado muito mais fácil a minha chegada e adaptação a Aveiro e também pelos momentos de diversão e de distração necessários durante estes dois anos.

Um muito obrigado a todos!

palavras-chave

Infeção viral; tRNA; tsRNA; Vírus Influenza A;

resumo

O vírus Influenza A (IAV) é um vírus respiratório que causa epidemias sazonais anuais e surtos pandémicos esporádicos. Anualmente, as epidemias causadas por estes vírus resultam em 1 bilião de infeções, 3-5 milhões de casos de doença grave e 300.000-500.000 mortes em todo o mundo, de acordo com a Organização Mundial de Saúde (OMS)

Os vírus são pequenos agentes infeciosos oportunistas que dependem da maquinaria das células do hospedeiro para se propagarem. Os vírus carecem de elementos-chave necessários para a replicação do seu genoma e para a tradução de proteínas virais, como os ácidos ribonucleicos de transferência (tRNAs). Os tRNAs são moléculas de RNA não codificantes com um papel fundamental na síntese proteica, pois convertem a informação presente no mRNA em cadeias de péptidos. Recentemente, uma nova classe de moléculas de RNA não codificantes derivadas de tRNAs foi identificada. Esta classe é conhecida como pequenos RNAs derivados de tRNA (tsRNAs) e é originada pela clivagem de moléculas de tRNA por endonucleases como a Dicer e a Angiogenina. A presença de tsRNAs foi confirmada em várias doenças, desde vários tipos de cancro a infeções virais. Embora ainda não seja claro se os tsRNAs desempenham um papel ativo na patogénese das doenças, alguns destes tsRNAs são específicos para determinadas doenças.

Neste estudo, tentámos perceber se a Infeção por IAV leva à formação de tsRNAs e em que ponto específico da infeção isso ocorre. Os nossos resultados demonstraram que durante a infeção por IAV existe de facto formação de tsRNAs (5'-Gly-GCC tsRNAs e 5'-Glu-CTC tsRNAs) e que a sua formação ocorre principalmente 2 a 4 horas após a infeção. Também analisámos a possibilidade da angiogenina ser a enzima responsável pela formação dos tsRNAs observados e se a presença de 5'-Gly-GCC tsRNA tem algum efeito na infeção por IAV. Os nossos resultados sugerem que esta enzima não é a responsável pela formação dos tsRNAs detetados e que o aumento de 5'-Gly-GCC tsRNA não teve efeito na formação de partículas infeciosas de IAV.

keywords

Viral infection; tRNA; tsRNA; Influenza A virus;

abstract

Influenza A virus (IAV) is a respiratory virus that causes yearly seasonal epidemics and sporadic pandemic outbreaks. Annually, influenza epidemics result in 1 billion infections, 3–5 million cases of severe disease, and 300,000–500,000 deaths worldwide, according to the World Health Organization (WHO).

Viruses are small opportunistic infectious agents that rely on the host cells machinery to propagate. Viruses lack, among others, key elements for genome replication and viral protein translation such as transfer ribonucleic acids (tRNAs). tRNAs are non-coding RNAs (ncRNAs) with a key role in protein synthesis, as they convert the information from mRNA into a peptide chain. Recently, a novel class of small ncRNAs (sncRNAs) derived from tRNAs, was identified. These are known as tRNA-small derived RNAs (tsRNAs) and are originated by cleavage of tRNAs by endonuclease enzymes like Dicer and Angiogenin. The presence of tsRNAs has been found in several diseases, ranging from cancer to viral infection, and, although it is still not clear whether tsRNAs play an active role in disease pathogenesis, some tsRNAs are disease specific.

In this study, we aimed to determine whether, and at which infection stage, IAV infection leads to the formation of tsRNAs. Our results demonstrated that IAV infection leads to the formation of tsRNAs, namely 5'-Gly-GCC tsRNAs and 5'-Glu-CTC tsRNAs, mainly at 2 hours post-infection and at 4 hours post-infection. We also analysed whether angiogenin would be the responsible enzyme for the formation of the observed tsRNAs and if the presence of 5'-Gly-GCC tsRNA would affect IAV infection. Our results suggest that this enzyme is not the main responsible for the formation of these specific tsRNAs and that the increase of 5'-Gly-GCC tsRNA did not affect the formation of infections IAV particles.

List of Abbreviations

-ssRNA	negative-sense single-stranded RNA
AGO	Argonaute proteins
ALS	Amyotrophic Lateral Sclerosis
APOER2	Apolipoprotein E Receptor 2
BCAR3	Bovine Cancer Anti-Estrogen Resistance 3
BSA	Bovine Serum Albumin
CARD	Caspase Activation and Recruitment Domains
ccRCC	clear cell Renal Cell Carcinoma
CRM1	Chromosomal Maintenance 1
cRNA	complementary RNA
CTL	Cytotoxic T Lymphocyte
DAPI	4’,6-diamidino-2-phenylindole
dH2O	Distilled Water
DMEM	Dulbecco's Modified Eagle Medium
DNA	Deoxyribonucleic Acid
EBC	Early-Breast Cancer
elF4F	eukarytotic Initiation Factor 4F
FBS	Fetal Bovine Serum
GISRS	Global Influenza Surveillance and Response System
HA	Haemagglutinin
HA1	Haemagglutinin subunit 1
HA2	Haemagglutinin subunit 2
HIV-1	Human Immunodeficiency virus 1 (HIV-1)
HPI	Hours Post-infection
HTLV-1	Human T-cell Leukemia virus type 1
HUVECs	Human Umbilical Vein Endothelial Cells
IAV	Influenza A virus
IFN	Interferon
IFN-β	Interferon-β
IRF3	Interferon Regulatory Factor 3
IRF7	Interferon Regulatory Factor 7
itRF	internal-tRNA-derived fragment
La	Lupus autoantigen
lncRNA	long non-coding RNA
M1	Matrix Protein
M2	Membrane Protein

MA2	Matrix 2
MAVS	Mitochondrial Antiviral Signalling proteins
MHC	Major Histocompatibility Complex
miRNA	micro-RNA
MRI	Magnetic Resonance Imaging
mRNA	messenger RNA
mRNP	messenger Ribonucleoproteins
NA	Neuraminidase
ncRNA	non-coding RNA
NEP	Nuclear Export Protein
NF-κB	Nuclear Factor kappa-light-chain-enhancer of activated B cells
NK	Natural Killer
NLRP3	NOD-like Receptor Family Pyrin domain containing 3
NLS	Nuclear Localization Signals
NP	Nucleoprotein
NS1	Non-structural Protein 1
NS2	Non-structural Protein 2
P/S	Penicillin/Streptomycin
PA	Acidic polymerase
PAMP	Pathogen-associated Molecular Pattern
PB1	Basic polymerase 1
PB2	Basic polymerase 2
PBS	Phosphate Buffered Saline
PCH	Pontocerebellar Hypoplasia
pDC	plasmacytoid Dendritic Cells
PFA	Paraformaldehyde
piRNA	piwi-interacting RNA
PKR	RNA-dependent protein kinase
PRR	Pattern-recognition Receptor
RBP	RNA-binding proteins
RIG-I	Retinoic acid-inducible gene-I
RISC	RNA-induced Silencing Complex
RNA	Ribonucleic Acid
RNP	Ribonucleoprotein
rRNA	ribosomal RNA
RSV	Respiratory Syncytial Virus
RT-qPCR	Reverse Transcription-Quantitative Polymerase Chain Reaction
SA	Sialic Acid

SFM	Serum Free Medium
SG	Stress granule
siRNA	small interfering RNA
sncRNA	small non-coding RNA
tiRNA	tRNA-derived stress-induced RNA
TLR	Toll-like Receptor
TLR3	Toll-like Receptor 3
TLR7	Toll-like Receptor 7
TLR8	Toll-like Receptor 8
TLR9	Toll-like Receptor 9
tRF	tRNA-derived fragment
TRIF	TIR-domain-containing adapter-inducing IFN-β
TRIM25	Tripartite Motif Containing 25
tRNA	transfer RNA
tsRNA	tRNA-derived small RNA
UTR	untranslated region
vRdRp	viral RNA-dependant RNA polymerase
vRNA	viral RNA
vRNP	viral Ribonucleoprotein
VSMCs	Vascular Smooth Muscle Cells
WHO	World Health Organization

List of figures

Index

Chapter I – Introduction

1.1 Influenza viruses

Influenza is an infectious respiratory disease caused by influenza viruses. Currently, there are four types of influenza viruses: A, B, C, and D. Most cases of Influenza are due to the influenza A virus (IAV) and influenza B virus, although the majority is induced by IAV[1]. Influenza C virus does not cause substantial disease in humans, only causing influenza-like illness, especially in children[2]. Influenza D virus infection has never been observed in humans[3].

1.1.1 Influenza A virus genome and morphology

IAV belongs to the Alpha influenza virus genera, from the Orthomyxoviridae family. IAV has various subtypes, based on its two major surface proteins, haemagglutinin (HA) and neuraminidase (NA). There are 18 HA types (H1 to H18) and 11 NA types (N1 to N11) discovered and identified until now[4].

Morphologically, IAV particles are spherical or filamentous in shape. The IAV spherical particles have around 100 nm in diameter and the filamentous forms often exceed 300 nm in length[5,6].

The viral genome is composed of eight RNA segments that encode RNA polymerase subunits, viral glycoproteins (HA and NA), matrix protein (M1) and membrane protein (M2), the non-structural protein NS1, and nuclear export protein (NEP) (**Figure 1**)[7].

The viral capsid is enclosed in a lipid envelope derived from the cellular membrane of the host cell. The viral proteins HA and NA are inserted in this lipid envelope in a 4:1 ratio of HA to NA proteins[6,8]. M2 ion channels are also present in the envelope but are a minor component, with only 16 to 20 molecules per virion[8,9]. The lipidic envelope and its proteins overlay a matrix of M1 protein, enclosing the virion core[5,6] that consists of viral ribonucleoproteins (vRNPs) made up of viral RNA (vRNA) wrapped around viral proteins like NP and NEP[8].

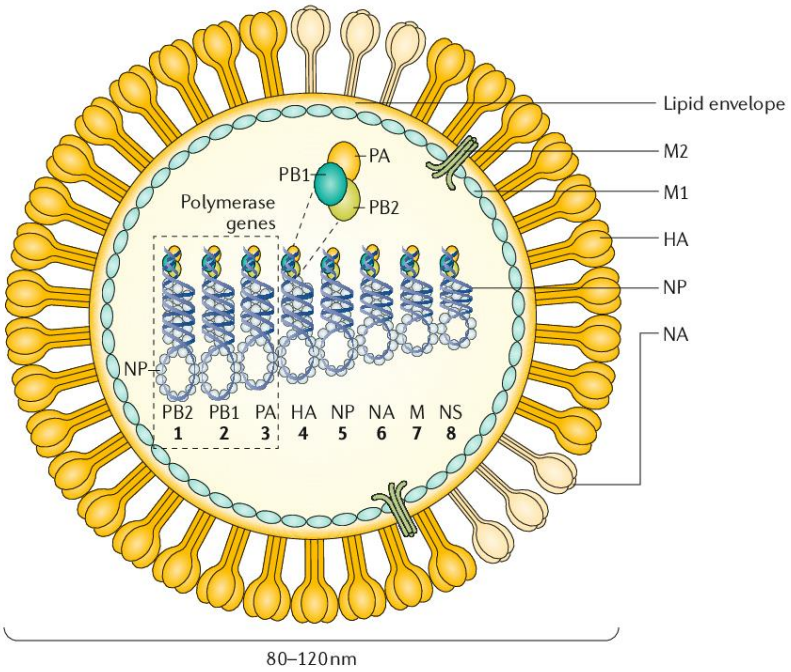

Figure 1 – Schematic representation of an Influenza A virus particle. Krammer et al. 2018[7]**.**

The eight viral negative-sense single-stranded RNA (-ssRNA) segments are numbered, in decreasing length (**Figure 1**), with segment 1 having 2341 nucleotides and segment 8 having 890 nucleotides[10].

The three largest RNA segments (segment 1, 2 and 3) encode the three subunits of vRNA-dependent RNA polymerases (PB1, PB2, and PA), which are in charge of RNA synthesis and replication in infected cells[6,7].

Segments 4 and 6 encode the viral glycoproteins HA and NA, respectively. The first mediates viral entry and binding to sialic acid-containing receptors, while the second is responsible for releasing viruses bound to non-functional receptors and assisting viral spread[6,7].

The viral nucleoprotein (NP), encoded by RNA segment 5, is responsible for the binding of the RNA genome and, together with the vRNA-dependent RNA polymerase, forming the ribonucleoprotein (RNP) complex[10]. NP is also involved in nuclear import and export regulation[8]. RNA segment 7 encodes the M proteins, M1 and M2, and segment 8 encodes the interferon-antagonist NS1 protein and the NEP (or NS2) involved in the RNP export from the nucleus of the host cell[6,7].

The M1 protein is thought to provide a scaffold that aids virion structure and, along with NEP, regulates the trafficking of vRNA segments in the cell while the M2 protein is a proton ion channel that is required for viral entry and exit[6,7].

The NS1 protein functions as a virulence factor in infected cells by inhibiting host antiviral responses (see section **1.1.3 Influenza A virus and host defences**)[6,7].

1.1.2 Influenza A virus life cycle

The IAV life cycle can be divided into five stages: **(1)** virus attachment and entry into the host cells; **(2)** entry of vRNPs into the nucleus; **(3)** transcription and replication of the viral genome; **(4)** synthesis of viral proteins; **(5)** assembly and budding at the host cell plasma membrane (**Figure 2**)[8].

(1) Virus attachment and entry

The HA protein found on the surface of the viral envelope is an essential part of the virus attachment and entry process. HA possesses two subunits, HA1 and HA2; while HA1 contains a receptor-binding domain, HA2 contains a fusion peptide[8]. Upon reaching a potential host, IAV recognizes N-acetylneuraminic acid or sialic acid (SA) on the host cell's surface. Following this, the HA receptor-binding site (HA1) attaches the virus to the surface glycoconjugates that contain terminal SA residues[5,10]. Human IAV HA-mediated binding favours a -2,6 linkage, resulting in a more "bent" presentation, whereas avian IAV has a stronger selectivity for -2,3-linked SA receptors, resulting in a more "linear" appearance[11].

After the attachment, the virion gets endocytosed. The acidity of the endosomal compartment is crucial for the virion uncoating. This acidity initiates a conformational change in the HA molecules at the surface of the viral envelope. The HA molecule exposes its H2 subunit and triggers the merge of the viral envelope with the endosomal membrane[12]. The low pH (around 5 or 6) will also activate the M2 ion channels, opening them and acidifying the inside of the viral particle, breaking protein-protein interactions and releasing the vRNPs from the M1 matrix into the host cells cytoplasm[13].

(2) vRNPs entry into the nucleus

The vRNPs entry into the nucleus for genome replication and transcription is dependent on the host cell transport pathways[10]. All the proteins that compose vRNPs, NP, PA, PB1, and PB2, have nuclear localization signals (NLSs) that bind to the cellular nuclear import machinery and, thus, enter the nucleus[8]. According to numerous studies, vRNPs use these NLSs to engage the importin-α–importin-β pathway, recruiting the adapter protein importin-α[14].

(3) vRNA synthesis (transcription and replication)

For the genome to be transcribed, the negative-sense RNA must get converted into positive-sense RNA, which will serve as a template to produce vRNAs[8]. Instead of using a primer, the genome replication uses the vRNA-dependent RNA polymerase (vRdRp), which exhibits partial inverse complementarity with the genome and is imported alongside the negative-sense RNA segments[8,10].

The vRdRp complex uses the RNA as a template to synthesize two different types of positive-sense RNA: messenger RNA (mRNA) produced by transcription, which will serve as a template for viral protein synthesis, and complementary RNA

(cRNA) intermediates produced by replication, from which more copies of the negative sense vRNA will be transcribed[10].

While mature cellular mRNAs have a 5' methylated cap and a poly(A) tail, the vRNPs have poly(A) tails but do not have 5' caps, a "cap-snatching" mechanism occurs for complete vRNA synthesis[15].

The vRdRp complex consists of 3 viral proteins: PB1, PB2, and PA. The viral polymerase uses the PB2 subunit to promote binding of the complex to the 5' methylated caps of the host's mRNAs. After binding, the viral polymerase uses the PA subunit to cleave the cellular pre-mRNAs 10 to 15 nucleotides from the cap structure. This capped RNA fragment is then used by the vRdRp, via the PB1 subunit, as a primer for viral transcription[5,8]. In contrast, the production of cRNA by replication does not need a primer to initiate[5].

(4) Synthesis of viral proteins (translation)

The synthesis of viral proteins takes place in the cytoplasm, upon export of capped mRNA from the nucleus.

The viral core proteins PB1, PB2, PA, NP, NS1, and NS2/NEP are translated from vRNAs in cytosolic ribosomes[10]. Since the assembly of the vRNPs occurs in the nucleus, the subunits of the vRNP complex (PB1, PB2, PA, and NP) are imported back to the nucleus after being synthesized[16,17]. The new vRNA segments are encapsulated by viral polymerase and NP. The newly formed vRNPs are then exported from the nucleus into the cytoplasm via the Cromossomal Maintenace 1 (CRM1) dependent pathway through the nuclear pores. M1 protein binds to the vRNPs and to NEP which, in turn, binds to CRM1. It's through this "daisy-chain" complex that the exportation from the nucleus takes place[8,17].

The proteins found on the viral envelope (HA, NA, and M2) are synthesized at the endoplasmic reticulum by membrane-bound ribosomes. These proteins are then folded and trafficked to the Golgi apparatus, where they will undergo post-translational modifications. All the viral envelope proteins have atypical sorting signals that direct them to the cell membrane for virion assembly[10].

(5) Virus packaging, assembly and budding

It was initially believed that the packaging of viral genome into the newly formed virus particles method was a random process, where vRNA segments were incorporated into budding vesicles and where only those with the eight different genome segments would become infectious. However, evidence shows that the packaging process is more selective, where discrete packaging signals on all vRNA segments ensure the incorporation of the entire genome in the virus particles[10]. The packaging signals have been identified at the 5' and 3' non-coding and coding regions of some of the viral segments[18].

IAV budding occurs at the cell membrane and gets initiated by the accumulation of M1 at this location. After budding is complete, HA protein keeps binding the virion to the SA present on the cell's surface[10]. One of the most significant steps is the

cleavage of the SA residues from glycoproteins and glycolipids through the sialidase activity of the NA protein[8]. NA also removes SA residues from the virus envelope, preventing the aggregation of viral particles[10].

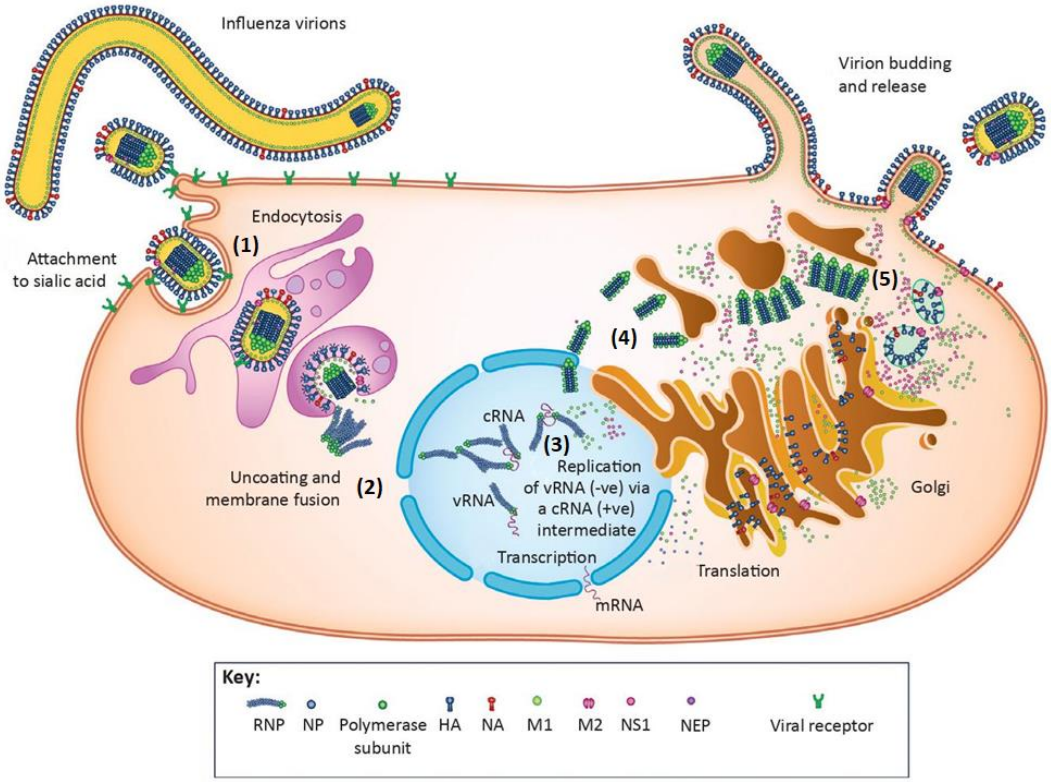

Figure 2 – Schematic representation of the IAV life cycle. (1) IAV enters the host cells by attachment and entry through recognition of SA by HA molecules on the viral envelope, and endocytosis. **(2)** VRNPs enter the nucleus through NLSs, activating the the importin-α–importin-β import pathway. **(3)** vRNA is synthesized in the nucleus, using the vRdRp complex as a template for mRNA and cRNA. **(4)** Production of viral proteins through translation of viral mRNA, using the hosts translation machinery, in the cytoplasm and endoplasmatic reticulum. Some may suffer post-translation modifications in the Golgi apparatus. **(5)** Virus packaging, assembly and budding near the cell membrane and release of the new virus particles. Adapted from Hutchinson (2018)[4].

1.1.3 Influenza A virus and host defences

The initial line of defence against IAV infection is the innate immune system. It consists of components, such as mucus and collectins, that work to keep the respiratory epithelial cells from becoming infected. Furthermore, fast innate cellular immune responses are elicited to limit viral replication[19].

Pattern-recognition receptors (PRRs) are proteins with the ability to recognize molecules frequently found and associated with pathogens. For IAV, its main pathogen-associated molecular pattern (PAMP) is its vRNA. The recognition of vRNA by these PRRs will activate the innate immune system signals that induce the production of various cytokines and antiviral molecules[19,20].

The PRRs involved in IAV recognition are toll-like receptors (TLRs), the retinoic acid-inducible gene-I (RIG-I), and the NOD-like receptor family pyrin domain containing 3 (NLRP3) protein. TLRs are present at the surface of endosomes and lysosomes, being TLR 3, TLR 7, TLR 8 and TLR 9 the ones involved in IAV recognition[19]. RIG-I is the principal receptor for intracellular -ssRNAs and transcriptional intermediates in infected cells[20]. NLRP3 protein is a PRR but is also a component of the NLRP3 inflammasome, a cytoplasmic complex related to influenza virus immunity[20].

After recognizing PAMPs, RIG-I exposes its caspase activation and recruitment domains (CARDs), which are then modulated by dephosphorylation or ubiquitination, by E3 ligases[20]. With this, the CARD-dependent association between RIG-I and the mitochondrial antiviral signalling proteins (MAVS) at mitochondria[21] and peroxisomes[22] triggers the downstream transduction signalling cascade, which continues with the activation of the interferon regulatory factor 3 (IRF3) and 7 (IRF7), and the nuclear factor kappa-light-chain-enhancer of activated B cells (NF-κB), leading to the expression of various interferons (IFNs) and cytokines[20].

TLR 7 and TLR3 are critical for detection of IAV infection. TLR7 binds to viral ssRNA, particularly in plasmacytoid dendritic cells (pDC), whereas TLR3 binds to double-stranded vRNA in most of the other infected cells. The activation of these receptors results in the release of proinflammatory cytokines and type I IFNs[19]. TLR7 activation induces interferon 7 (IRF7) production, which regulates the expression of other IFNs like Interferon-β (IFN-β). TLR3 also regulates the expression of IFN-β through its interaction with the TIR-domain-containing adapter-inducing IFN-β (TRIF)[19,20].

The NLRP3 inflammasome needs threes signals to be activated. Firstly, NLRP3 must be activated through pathogen detection, inducing the expression of pro-IL-1β, pro-IL-18, and pro-caspase-1. After this, M2 ion channel activity triggers the cleavage of pro-IL-1β and pro-IL-18[20]. The accumulation of IAV PB1-F2 in the lysosome is the third signal needed for the final activation of the NLRP3 inflammasome[20].

The respiratory tract epithelial cells are the main target of IAV after entering the human body. Macrophages and natural killer cells (NK cells) are prominent effector cells in the innate immune response. These cells can recognize antibody-bound influenza virus-infected cells and then phagocyte (in the case of macrophages) or lyse (in the case of NK cells) them, limiting the viral spread of IAV in the body[19].

The adaptive immune system functions as the body's second line of defence against IAV infections. It is composed of humoral and cellular immunity, mediated by virus-specific antibodies and T cells, respectively[19].

T cells and B cells play key roles in the adaptive immunity against IAV infection. T cells are classified as CD4+ and CD8+ T cells. CD8+ T cells mature into cytotoxic T lymphocytes (CTLs), which produce cytokines and effector molecules that limit viral replication and kill virus-infected cells[20]. The CD8+ T cells are activated by dendritic cells leading to their differentiation into CTLs[23]. Type I IFNs, like the ones released after TLRs activation, also help the differentiation of T cells[19,20].

CTLs create cytotoxic granules, including chemicals such as perforin and granzymes, after targeting virus-infected cells. Perforin attaches to target cells, forming pores on the cell membrane that allow granzymes to diffuse passively and induce apoptosis. Post-infection, the virus specific CTLs circulate through the blood and lymphoid organs in the body. These are memory CTL cells, and they will quickly respond to further IAV infections more proficiently and efficiently[20].

To establish a successful infection, IAVs have evolved multiple strategies to circumvent the host immunity, and NS1 protein seems to be a key player in this process, suppressing the host IFN response by binding to vRNA and masking it from RIG-I and TLR recognition[20,24].

The presence of vRNA in the hosts' cells causes ubiquitination of RIG-I by Tripartite Motif Containing 25 (TRIM25), activating the pathway, and triggering innate immunity. However, NS1 can bind to TRIM25, blocking RIG-I activation[20]. Instead of blocking RIG-I activation, it can also form a complex with RNA-dependent protein kinase (PKR), blocking its function[19]. PKR would usually lead to the production of IFNs and inhibition of viral protein synthesis[19,20].

Besides helping to avoid the host's innate immunity, NS1 also influences adaptive immunity by modulating the maturation and capacity of dendritic cells to induce T-cell responses[25].

1.1.4 Influenza viruses and epidemiology

While Influenza is typically characterized by yearly seasonal epidemics, sporadic pandemic outbreaks involving IAV strains of zoonotic origin occur occasionally. Annual influenza epidemics result in 1 billion infections, 3–5 million cases of severe disease, and 300,000–500,000 influenza-related deaths worldwide, according to the World Health Organization (WHO)[7].

Symptoms of influenza virus infection range from a mild upper respiratory disease characterized by fever, sore throat, runny nose, cough, headache, muscle pain, and fatigue to severe and, in some cases, lethal pneumonia caused by influenza viruses or secondary bacterial infection of the lower respiratory tract[26].

IAV spreads through aerosols and causes an acute febrile respiratory disease in humans known as "flu," which is more severe in small children, the elderly, and immunocompromised people[27].

The occurrence of new influenza epidemics derives from its constant antigenic evolution since IAV is well equipped to promote antigenic diversity through either *antigenic drift* or *antigenic shift*[28]*. Antigenic* drift is a continuous process where mutations accumulate in HA and NA proteins, resulting in antigenic variants capable of re-infecting hosts while evading the antibodies granted by the previous exposure[28]. RNA viruses are in general more susceptible to *antigenic drift* since RNA is more unstable and prone to mutations than DNA. Along with natural selection and frequent reassortment, this is the principal cause of seasonal influenza epidemics[29]. *Antigenic shift*, on the other hand, is a sporadic event that, due to the segmented nature of the IAV genome, occurs when gene segments of different parental viruses, within the same host, get reassorted. Since this will cause a new combination of HA and NA proteins, it will disseminate quickly throughout the world, as no previous immunity exists in the population. *Antigenic shift* is associated with novel IAV pandemics[30]. The major contributor for *antigenic shift* in IAV is the broad range of animal reservoirs that provide antigenically diverse HA and NA genes. The first recorded IAV pandemic in 1918, the H1N1 IAV subtype, originated from a reassortment between a human H1 subtype and an avian N1 subtype[31].

The key to control viral pathogens is a trio of surveillance, antiviral drugs, and vaccination, and the same applies to IAV.

Vaccines are at the forefront of efforts to prevent and control the spread of IAV infections. Due to *antigenic shift* and *antigenic drift*, the high variability of HA and NA antigens makes it impossible to develop a universal vaccine. However, vaccines specific to individual influenza viruses are available and have advanced significantly in matters of composition and administration since their initial introduction in the 1940s[32]. Numerous studies have found that the effectiveness of influenza vaccines varies in three different ways: it appears to vary from season to season, to vary by age group from season to season, and to vary with vaccination history[33]. Seasonal IAV vaccines are reformulated, manufactured, and distributed for administration to the global human population each year, soon before the start of flu season, as a prevention method to IAV infection[34]. This process is based on a worldwide surveillance effort in the Northern and Southern hemispheres sponsored by the WHO, namely through the Global Influenza Surveillance and Response System (GISRS)[35].

Antiviral drugs play a significant role in treating IAV-induced sickness. Antiviral drugs can have therapeutic and prophylactic effects, but they must be administered continuously during high influenza activity to prevent disease[30]. Currently, there are two classes of drugs approved for influenza treatment: adamantanes and NA inhibitors. Adamantanes, like amantadine and rimantadine, target the Matrix 2 (MA2) ion channels. Adamantanes bind to MA2 ion channels blocking them and preventing the release of vRNP. These drugs are effective against IAV, but some resistant viral strains started to develop rapidly. At this point, adamantanes are no longer recommended globally due to widespread resistance among the circulating IAV strains, being recognized in approximately one-third of treated patients[7,30]. On the other hand, NA inhibitors like zanamivir and oseltamivir, are effective against influenza A and B viruses. NA inhibitors target the enzymatic activity of the viral NA protein, leading to the aggregation of viral particles on the host cell surface preventing the release of newly formed virions[36]. These drugs are effective when administrated prophylactically[30].

1.2 Transfer RNAs (tRNAs)

RNAs are divided into two main categories, coding RNAs and non-coding RNAs (ncRNAs). mRNA is the only class of coding RNAs. These mRNAs carry the genetic information that will be translated into proteins. On the other hand, ncRNAs do not encode any proteins and have diverse functions[37].

The ncRNAs can be further classified into long non-coding RNAs (lncRNAs, >200 nucleotides) and small non-coding RNAs (sncRNAs, <200 nucleotides), depending on the size of the ncRNA molecule[37,38]. The sncRNAs include housekeeping RNAs, namely ribosomal RNAs (rRNAs), small-nuclear RNAs and tRNAs; and regulatory RNAs, such as piwi-interacting RNAs (piRNAs), and micro-RNAs (miRNAs), among others[38,39].

Transfer RNAs (tRNAs) are sncRNAs with a key role in protein synthesis, as they convert information from mRNA into peptide chains, by recognizing the mRNA codons and ensuring the incorporation of the correct amino acid into the nascent polypeptide[40]. This is considered the canonical role of tRNAs but cumulative evidence shows that they can also perform other noncanonical functions, namely, regulatory functions and as precursor molecules[40].

Mature tRNAs are usually 70-90 nts long and have a well-conserved cloverleaf-like secondary structure[41]. This secondary structure can be divided into five different parts: the acceptor stem (with the 5'- and 3'- ends), the D-arm, the TΨC-arm (or T-arm), the variable loop, and the anticodon-arm (where the anticodon is located). A CCA sequence is added to the 3'-end of all mature tRNAs, acting as the site of amino acid attachment[42]. The tertiary structure of tRNAs is L-shaped and is maintained through hydrogen bonds and stabilized mostly through interaction between the D- and the T-arms[43].

tRNA biogenesis starts in the nucleus when the RNA polymerase III transcribes the tRNA as a pre-tRNA, a precursor molecule. The pre-tRNA will then be processed into the mature tRNA[44].

Firstly, the leader sequence is cleaved and removed by the RNaseP enzyme, followed by the cleavage and removal of the trailer sequence by the RNaseZ enzyme. Afterwards, the CCA tail is added to the 3'-end of the maturing tRNA molecule by a CCA-adding enzyme, the CCA nucleotidyltransferase. The existing introns are then spliced, and the mature tRNA molecule is ready to be exported to the cytoplasm where it is subjected to post-transcriptional modifications by tRNA-modifying enzymes. Also at the cytoplasm, the mature tRNAs are charged with the corresponding amino acid by aminoacyl-tRNA synthetases, which will be added to the CCA tail previously added to the 3'-end. This process is known as aminoacylation and, after it, the charged tRNA is ready to be a part of the protein synthesis machinery[44,45].

1.2.1 tRNA-derived small RNAs

The development of more powerful high-throughput sequencing technologies and microarrays allowed a more thoughtful insight into sncRNAs. These technologies clarified that there are many more classes than initially predicted, including sncRNAs derived from tRNAs through cleavage and processing[46,47]. These novel sncRNAs are known as tRNA-derived small RNAs (tsRNAs), and their role and function are only now starting to become understood, as they are specifically produced in certain situations and are not only by-products of tRNA degradation[48].

tsRNAs are produced through specific cleavage of tRNAs by endonuclease enzymes like Angiogenin, Dicer, and ELAC2[47,49]. These tsRNAs forming enzymes cleave the tRNA in different places, forming fragments of different dimensions, originating different tsRNA sub-classes, namely, tRNA-derived fragments (tRFs) through cleavage by dicer, tRNA-derived stress-induced RNAs (tiRNAs) through cleavage by angiogenin and internal-tRNA-derived fragments (itRFs) (**Figure 3**)[49,50].

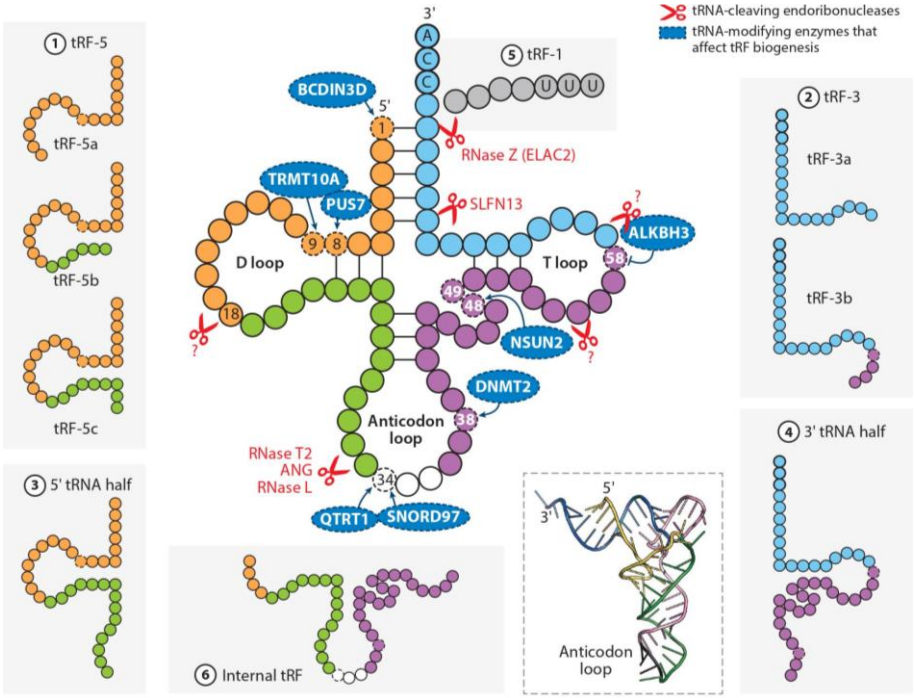

Figure 3 – Schematic representation of the biogenesis and classification of the various types of tsRNAs. There are six major types of tsRNAs: they can be divided into tRFs (tRF-5, tRF-3 and tRF-1), itRFs, and tRNA halves (5' or 3') also known as tiRNAs. Each type of tsRNA is processed from mature tRNA or pre-tRNA and has a distinct biogenesis pathway generated by different ribonucleases (shown in red). Adapted from Su et al. 2020[40].

Depending on where the tRNA cleavage takes place and on the location of the fragment in the precursor tRNA, the tRFs are divided into three main subclasses, which include tRF-5, tRF-3 (derived from the 5' and 3' ends), and tRF-1 (derived from the pre-RNA trailer sequence)[51]. Both tRF-5 and tRF-3 are originated by Dicer and are a product of the cleavage of mature tRNA in the D-arm and T-arm, respectively[47,51]. The tRF-1,

however, is derived from the 3'-end of the pre-tRNA. Therefore, tRF-1 consists of the trailer sequence that is removed during the maturation process[48]. The cleavage of the 3'-end of pre-tRNAs occurs due to the RNase Z enzyme and is the least abundant of the three.

tRF-5s exhibit a regular pattern, having a length of 14 to 32 nts. These fragments can be classified further into tRF-5a (14–16 nt), tRF-5b (22–24 nt), and tRF-5c (28–30 nt), based on the different cleavage sites in the D-loop or the stem region between the D-loop and the anticodon loop in the tRNA[52].

itRFs or tRF-2, are tsRNAs generated by cleavage of the anticodon loop of mature tRNAs, the internal arm of the tRNA[50]. These are the most uncommon subclass of tsRNAs[53].

The tiRNAs have a much bigger size (30-50 nts) and are generally originated by angiogenin cleavage near the anticodon. These tiRNAs are mainly formed in response to stress, including virus infection or hypoxia[49]. Since angiogenin cleaves the tRNA at or near the anticodon, tiRNAs are also known as tRNA halves[50].

Until this point, a consensus nomenclature and classification of tsRNAs is still rudimentary, with an almost frequent change and overlap in terms due to new characteristics and functions still being discovered[54]. During this study, we will refer to the various types of tsRNAs as previously described.

1.2.2 tsRNAs in disease

tsRNA production was observed in various diseases, but it is still unknown whether they actively play a role in disease pathogenesis[55]. Nevertheless, some tsRNAs can be helpful biomarkers, as some are produced only during specific stress conditions or in particular diseases[56,57].

In pathological stress-related injuries, tsRNAs have been shown to serve as a reliable biomarker whose production was correlated with tissue damage[58]. Oxidative stress may induce changes in tRNA conformations, which promotes the production of tRNA halves by angiogenin cleavage. This changes in conformation result in an exposition of 1-methyladenosine nucleoside (m1A), which gets recognized by an m1A-specific antibody (anti-M1A). In humans, m1A antibody recognition showed that cisplatin-mediated nephrotoxicity generated tiRNAs in the damaged kidneys, proving that stress-related injuries lead to the production of tiRNAs[58].

Neurodegenerative diseases have been linked to tRNA metabolism and tRNA processing enzymes, as the cause of several neurological disorders like pontocerebellar hypoplasia (PCH). Since tsRNAs have also been linked to tRNA metabolism and processing, a link between tsRNAs and neurological diseases is now being studied[59]. Since 2006, angiogenin mutants with reduced RNase ability have been continuously associated with the pathogenesis of Amyotrophic Lateral Sclerosis (ALS); later, a subset of the same angiogenin mutants was also linked to Parkinson's Disease[59,60]. The mutations found caused RNase loss of function, which may impact tiRNA formation. Overall, the wild-type angiogenin may play a protective role against stress and neurotoxins, with the possibility that angiogenin-dependent tiRNAs may contribute to motor neuron survival through inhibition of apoptosis[61,62]. tiRNAs have already been identified to be involved in

apoptosis via two mechanisms. The first is by interaction with Cytochrome C inhibiting the apoptosome formation. The second approach is to induce tRNA processing enzymes to cleave apoptosis-related mRNAs[62]. The last could result in a possible therapy application.

Cancer cells possess a higher metabolism than normal cells and, consequently, protein synthesis components and the protein translation machinery, are also adjusted to this higher metabolic demand. Because of this, cancer cells have a higher level of rRNAs, tRNAs, and ribosomes than non-tumoral cells[63].

Angiogenin is over-expressed in almost all types of cancer since it induces tumor angiogenesis and promotes cancer cell proliferation. Angiogenin ribonuclease activity is critical for the initiation of angiogenesis[64] and tiRNA production[49]. Whether the increase in tRNA levels leads to an increase of tiRNAs in cancer cells is still unknown but, it is possible that tiRNAs directly contribute to angiogenin-mediated angiogenesis and cancer cell proliferation[55]. tiRNAs can also help cancer cell survival by preventing apoptosis, binding to cytochrome C[62].

On prostate cancer, the lack of tRF-1001, a tRF derived from pre-tRNASer, leads to suppression of DNA biosynthesis and cell proliferation[55]. This tRF is produced by cleavage of pre-tRNA by ELAC2, making it a susceptibility gene of prostate cancer, as its levels are directly related to cellular proliferation[65]. tRF-1001 is also expressed in various other cancer cell lines.

Recent studies revealed that tsRNAs can be found in circulation, avoiding degradation in the blood because of an association with circulating exosomes[58] showing that tsRNAs have the potential to be promising biomarkers for prognosis and diagnosis of cancers[57].

In the case of breast cancer, the most common screening methods are mammography, ultrasound, and magnetic ressonance imaging (MRI)[66]. All these methods only detect tumors with a minimum volume, risking missing early-stage cancer. Recently the abundance of six tsRNAs was found significantly decreased in plasma samples of early-breast cancer (EBC) patients when compared to normal controls[67], confirming the potential of these molecules as biomarkers.

tsRNAs have been recently linked to viral infections, with their induction being virus specific[68]. In 2013, Wang et al. discovered, through deep sequencing of cells infected with the human respiratory syncytial virus (RSV), that infection results in the abundant synthesis of tsRNAs[68]. This tsRNA, which derives from tRNAGlu(CTC), binds to and inhibits the expression of apolipoprotein E receptor 2 (APOER2). APOER2 is an anti-RSV protein, meaning that its inhibition enhances RSV replication[56].

Human T-cell leukemia virus type 1 (HTLV-1) and Human Immunodeficiency virus 1 (HIV-1) have also been linked to tsRNAs. tRF-3019 has been found to be entirely complementary to the primer binding site in HTLV-1 retroviral RNA[69]. It was also found that a tRF-3 can target the HIV-1 virus via RNA interference, and that tRF-3 cellular prevalence is positively linked with HIV-1 proliferation[70].

1.2.3 Functions of tsRNAs

Some tsRNAs have been shown to affect cells, mainly by interacting with protein translation, gene silencing, and protein sequestration[40].

It was shown that tsRNAs have both positive and negative impacts on translation regulation. By displacing eukaryotic initiation factor 4F (eIF4F) from mRNAs, tsRNAs inhibit mRNA translation. Furthermore, translation inhibition causes polysome disassembly, resulting in an influx of untranslated messenger ribonucleoproteins (mRNPs). This influx will, in turn, promote the formation of stress granules (SG) in the liquid phase by interacting with Y-box-binding protein 1 (YBX1), which plays a key role in the process[49]. However, a small number of reports associate tsRNAs, mainly tRFs, to protein translation promotion. For instance, tRF-3011b, derived from tRNALeu, promotes ribosome biogenesis by base-pairing itself with ribosomal protein mRNAs, enhancing its translation[71].

Some tsRNAs bind to Argonaute (AGO) proteins and have been proposed to have miRNA-like functions, specifically in post-transcriptional gene regulation[52,72]. tsRNAs have also been found in RNA-induced silencing complex (RISC), alongside complementary target mRNA. This seems to indicate that they can indeed silence genes through base-pairing just like miRNAs. tsRNAs have also been shown to interact with PIWI proteins and, besides interacting with AGO1/2, tsRNAs were observed interacting with PIWIL2[73]. With that being said, it is worth mentioning that, thus far, the majority of studies have predicted tsRNA targets using miR-target methods[40], causing a natural overlap in miRNA and tsRNA targets.

Another pathway tsRNAs can use to regulate gene expression, either by promoting or inhibiting it, is by sequestering RNA-binding proteins (RBP) from other RNAs. As mentioned above, some tsRNAs can interact with YBX1, suppressing the stability of several transcripts by inducing displacement of their 3’ untranslated region (UTR) from YBX1 that is required transcript stabilization[74]. Lupus autoantigen (La) is an RBP known to stabilize RNA Polymerase III transcripts, including pre-tRNAs and some vRNAs. Recently, it was discovered that La interacts with tsRNAs, which sequester La from vRNAs that employ it as a chaperone to enhance viral gene expression[75].

1.2.4 The effect of various 5’-Gly-GCC tsRNAs and 5’-Glu-CTC tsRNAs in disease

tRNAGly-derived tsRNAs are shown to be regularly present in cells under stress conditions. 5’-Gly-GCC tsRNAs have been shown to inhibit protein translation[76] regulate MERVL target[77], and inhibit cell proliferation[78]. In ischemic injury, the expression of a 5’-Gly-GCC tiRNA was upregulated when compared to normal cells[78]. In all cases, the induction of 5’-Gly-GCC tiRNAs resulted from angiogenin cleavage, making it angiogenin-dependent[54,78–80]. All this suggests that 5’-Gly-GCC tiRNAs may have a significant biological role linked to angiogenin, as well as be a useful biomarker.

Another work showed that 5’-Gly-GCC tsRNA is linked to high cytotoxicity in RNH1-knockout HeLa cells. RNH1 inhibits the ribonuclease/angiogenin inhibitor in HeLa cells. The elevated ribonucleolytic activity of angiogenin leads to the high production of tsRNAs, where 66% of those were 5’-Gly-GCC tsRNAs. At around 3 µM concentrations, this 5’-Gly-GCC tsRNA was highly cytotoxic, with cell viability as low as 15%[79].

Using deep sequencing and bioinformatic analyses, Li et al.[78] identified a 5'-Gly-GCC tiRNA that was one of the most abundantly found tsRNAs in ischemic rat brain. After ischemia induction, the level of this 5'-Gly-GCC tiRNAs increased significantly compared to non-ischemic cells, indicating that these fragments may have a regulatory role in ischemic pathophysiology[78]. In the same study, it was noticed that this same 5'-Gly-GCC tiRNA could also affect angiogenesis by profoundly inhibiting the proliferation, migration, and tube formation of endothelial cells. All this indicates that this tiRNA can inhibit angiogenesis by preventing or slowing down tissue regeneration[78].

A different 5'-Gly-GCC tsRNA may possess a role in atherosclerosis. This particular 5'-Gly-GCC tsRNA promotes cell adhesion, proliferation, and migration of Human Umbilical Vein Endothelial Cells (HUVECs) and Vascular Smooth Muscle Cells (VSMCs) by negatively regulating the protein expression of the Major Histocompatibility Complex (MHC)[81], a key player in the immune system.

During RSV infection in A549 cells, Wang et al. found that a 5'-Gly-GCC tsRNA was abundantly produced[68]. Although its function in RSV has not been identified yet, one other tRNAGly-derived tsRNA has been shown to have a gene trans-silencing function in RSV like miRNAs, but with different regulatory mechanisms, targeting anti-virus proteins and favouring RSV replication, contributing to RSV-induced inflamation[82].

The RSV specific 5'-Glu-CTC tsRNA is one of the most well understood tsRNAs when it comes to RSV infection. When this respiratory infection occurs, the production of this specific tsRNA increases through angiogenin cleavage, which promotes RSV replication due to its trans-silencing activity[68]. Later, it was foud that APOER2 was one of the silencing targets of this 5'-Glu-CTC tsRNA. The trans-silencing effect happened through binding of the 3'-portion to a target site in the 3'-untranslated region of APOER2, suppressing its expression. APOER2 was found to be an anti-RSV protein, hence, elevated 5'-Glu-CTC tsRNA expression would be beneficial to RSV replication[56]. The trans-silencing activity of this 5'-Glu-CTC tsRNA turned out to be dependent on AGO1 and AGO4, working as a mediator for the interaction between it and its targets. Even though all of this happens in RSV infection, AGO4 seems to have an important role as an antiviral factor during viral infections, including infections by IAV[83].

In ovarian cancer cells, a 5'-Glu-CTC tsRNA was shown to inhibit cancer cell proliferation. This 5'-Glu-CTC tsRNA directly binds to a 3'-untranslated region of the Breast Cancer Anti-Estrogen Resistance 3 (BCAR3) mRNA, a cell proliferation promoter, downregulating its expression and thus inhibiting the cancer cell proliferation[84].

There are 5'-Glu-CTC tiRNAs with the potential to be a non-invasive biomarker in clear cell renal cell carcinoma (ccRCC). This 5'-Glu-CTC tiRNA was identified as one of the tsRNAs with lower production when comparing with normal cells. The lower level of this 5'-Glu-CTC tiRNA was directly related to adverse clinical-pathological parameters, suggesting that this tiRNA has an important role in ccRCC pathogenesis regulation and that it can be used as a novel biomarker[85].

In sum, these results demonstrate that both 5'-Gly-GCC tsRNAs and 5'-Glu-CTC tsRNAs are two of the most abundantly expressed tsRNAs in cells under stress conditions and diverse pathological conditions, making them promising targets to study[86].

Chapter II – Goals of the Study

Most studies on tsRNAs focus on their potential as prognostic and diagnostic biomarkers, with just a small portion focusing on tsRNAs as potential therapeutic targets. In either case, most studies are related to their involvement in cancer, namely hepatocelular carcinoma[71], breast cancer [67,63] and prostate cancer[87].

In the context of viral infections, the more relevant information pertains to RSV infection[68,82] and T-cell leukemia virus type I infection[69]. RSV is the only virus where the role of tsRNAs is relatively well known, as previously mentioned in the introduction section[56,72].

To our knowledge, the relevance of tsRNAs during IAV infection was not previously explored.

The main goal of this project was to determine whether IAV infection leads to the production of tsRNAs, particularly 5'-Gly-GCC tsRNAs and 5'-Glu-CTC tsRNAs, in A549 cells. More specifically, at which time-point of IAV infection these tsRNAs are produced, and if they play a role in the ability of IAV to infect cells, to infer on the potential of these tsRNAs as putative therapeutic targets to tackle IAV infection.

Chapter III - Materials and Methods

3.1 Materials

3.1.1 Cell lines

- A549 (Adenocarcinomic human alveolar basal epitelial cells)
- MDCK (Madin-Darby Canine Kidney cells)

3.1.2 Viruses

- Influenza A virus PR8 (Strain A/Puerto Rico/8/1934 H1N1)

3.1.3 Cell culture stock solutions

- Dulbecco's Modified Eagle Medium (DMEM): High Glucose, with L-Glutamine and without Sodium Pyruvate, from Gibco™
- Penicillin/Streptomycin (P/S), from Gibco™
- Fetal Bovine Serum (FBS), qualified and E.U.-approved, from Gibco™
- Dulbecco's Phosphate Buffered Saline (PBS), without Calcium and Magnesium, from BioWest
- TrypLE™ Express Enzyme (1X), phenol red, from Gibco™
- L-Glutamine, from Gibco™

3.1.4 Antibiotics

- Penicillin/Streptomycin (P/S)

3.1.5 Buffers and solutions

- 1% BSA → BSA 2% diluted in 1x PBS
- 4% PFA → 20 g PFA in 450 ml ddH_2O, 4 drops 1 M NaOH, 50 ml 10x PBS
- 0,2%Triton X-100 → 0.2% Triton X-100 in 1x PBS
- Mowiol → 12 g Mowiol 4-88, 20 ml Glycerol, 40 ml PBS
- DMEM +/+ → DMEM supplemented with 10% FBS and 1% of P/S
- SFM → DMEM supplemented with 1% P/S
- 1x PBS (Non-Cell Culture) → 1.37 M NaCl, 80 mM $NaHPO_4$, 0.0268 M KCl, 0.0147 M KH2PO4, pH = 7.3, prepared from 10x PBS diluted in ddH2O
- Ethanol 70% → 70 ml of ethanol 100% and 30 ml of ddH2O
- MiliQ H_2O → RNAse free H2O
- 7% BSA → 0.7 g of BSA in 10 ml of ddH2O
- 1:1000 TPCK-Trypsin → 0.001 g of TPCK Trypsin in 1 ml of MiliQ H2O
- 2.4 % Avicel Solution → 2.4 g of Avicel powder in 100 ml of MiliQ H2O
- 1x Acid Wash Buffer → 1.35 M NaCl, 0.1 M KCl, 0.4 M Citric Acid, pH = 3, diluted in 180 ml of ddH2O

- 0.1% Toluidine Blue in PFA 4% → 0.05 g of Toluidine Blue in 50 ml PFA 4%
- 10x TBE → 7,56 g of TrisBase, 3,85 g of boric acid, 0,651 g of EDTA and 70 ml MiliQ water
- Hybridization Buffer → 3,3 ml of 20x SSPE, 1 ml of 50x Denhardts solution, 1 ml of 10% SDS and 4,7 ml of MiliQ water
- Washing Buffer → 50 ml of 20x SSPE, 25 ml of 10% SDS and MiliQ water up to 500 ml
- Plaque assay medium → 25 ml of 2.4% Avicel, 25 ml of SFM, 1ml of 7% BSA and 50 µL of 1:1000 TPCK-Trypsin
- Acid-Phenol: Chloroform, from Thermo Fisher Scientific
- Loading buffer, from mirVana™ miRNA Isolation Kit
- UltraPure™ Urea, from Invitrogen™
- Acrylamide solution mix 19:1, from Pan Reac Applied Chem
- Ethanol 100%
- dH2O

3.1.6 Primary antibodies

- Anti-NP mouse antibody, from Santa Cruz Biotechnology, Inc.
- DAPI, from Hoechst

3.1.7 Secondary antibodies

- Alexa 488 mouse antibody, from Hoechst

3.1.8 Northern Blot

- 10% Polyacrylamide-Urea Gel → 21g Ultrapure Urea, 12,5 ml Acrylamid solution mix 19:1, 5ml TBE 10x and MiliQ water until tota volume of 50 uL
- DynaMarker®Prestained Marker for Small RNA Plus weight marker
- Hybond™-N+ nylon membrane

3.1.9 tsRNA probes for Northern Blot

- tsRNA_GluCTC 5'-[DY 782] GC CGA ATG CTA ACC ACT AGA CCA CCA [DY782]-3', from Eurofin Genomics
- tsRNA_GlyGCC 5'-[DY782] GA GAA TTG TAC CAC TGA ACC A [DY782]-3', from Eurofin Genomics

3.1.10 Kits

- mirVana™ miRNA Isolation Kit, from Life Technologies™
- High-Capacity RNA-to-cDNA™ Kit, from Applied Biosystems™

3.1.11 RT-qPCR Master Mix and Gene expression Assays

- TaqMan™ Gene Expression Master Mix - Applied Biosystems (by Thermo Fisher Scientific)
- Angiogenin - TaqMan ® Gene expression Assays from Applied Biosystems (by Thermo Fisher Scientific)
- GAPDH - TaqMan ® Gene expression Assays from Applied Biosystems (by Thermo Fisher Scientific)

3.1.12 Transfection mediums and mimics

- Lipofectamine™ 2000 Transfection Reagent, from ThermoFischer
- Opti-MEM™ Reduced Serum Medium, from Gibco™
- Synthetic 5'-Gly-GCC mimic (5'-GCAUGGGUGGUUCAGUGGUAGAAUUCUCGCCUG-3'), from Eurofins Genomics
- Synthetic Scramble-tsRNA (5'-GUGGUAGAGGUUGCUAUCU-3'), from Eurofins Genomics

3.1.13 Softwares

- Microsoft Excel 2016
- Zen 3.3 Blue Edition
- Image Studio Lite Version 5.2
- GraphPad Prism 9.1
- DeNovix DS-11 Software, DeNovix
- 7500 Software, Applied Biosystems

3.2 - Methods

3.2.1 - Cell culture and cell lines

The cell lines used in the experiments were A549 cells, adenocarcinomic human alveolar basal epithelial cells, and MDCK cells, Madin-Darby Canine Kidney cells. All the cell culture techniques were performed in a Biosafety level II room, where the cells were maintained in an incubator at 37,5˚C and 5% CO2 content.

3.2.2 - Cell plating

The desired number of cells for the experiments were plated on the day before. First, the medium was removed, and the cells were washed with PBS 1x. Gibco® TrypLE Express was then added to detach the cells from the culture dish (incubated for 5 mins at 37°C, 5% CO2). After that, the cells were collected in a falcon tube and centrifuged for 3 minutes at 1000 rpm, forming a pellet.

After the supernatant was removed, the cells were resuspended in 20 ml complete DMEM (DMEM Gibco®, supplemented with 10% FBS and 1% Pen-Strap). 10 µL of the suspended cells were placed in a Neubauer Chamber, to be counted.

Finally, the cells were plated and incubated for approximately 24h at 37°C, 5% CO2.

3.2.3 - Infection

A549 cells were plated in 10 cm culture dishes on the day before infection, including control cells (referred to as mock during the experiments). Glass coverslips (12 mm) were added to the culture dishes to be used later for immunofluorescence.

Firstly, the culture medium in which the cells were incubated was removed with a vacuum pump. The cells were then washed with PBS 1x to remove all residues of the previous medium, mainly FBS, as it can interfere with the virus entry into the cells. After the PBS was removed, a mix of IAV PR8 (with a MOI of 3) and Serum Free Medium (SFM) (DMEM supplemented with 1% Pen-Strap) was prepared in a falcon tube. 3,5 ml of the prepared mix was added to every culture dish except to our control. To the control dish, 3,5 ml of SFM, without any IAV PR8 virus, was added instead.

The culture dishes were then placed on a shaker for 5-10 minutes, at room temperature, to stimulate virus entry into the cells, followed by a 45-minute incubation at 37˚C, 5% CO2. After the incubation period, the SFM supplemented with 20% FBS was added to the culture dishes in the same volume as before (3,5 ml).

All the culture dishes were then incubated at the same conditions and the cells were harvested at the determined hours post-infection (2 hours, 4 hours, 6 hours, 8 hours, and 12 hours).

3.2.4 - Infected cell harvesting

At the determined time points, the cells were harvested. The cells' medium was removed with a vacuum pump, then 2 ml of Gibco® TrypLE Express was added to the cells. The cells were incubated for 5 minutes at 37˚C, 5% CO2, to detach them from the base of the culture dish. After the incubation period, the cells were collected to a 2 ml

Eppendorf and then centrifuged for 3 minutes at 3000 rpm, forming a pellet at the bottom.

The supernatant was discarded and 500 µL of PBS 1x was added to wash the pellet, followed by another 3 minutes centrifugation at 3000 rpm. The PBS was then discarded, and the cells were stored at -30˚C for posterior RNA extraction and isolation.

3.2.5 - Immunofluorescence

The 12 mm coverslips from the infection protocol were placed in a 24-well plate. The entire immunofluorescence protocol was performed at room temperature.

Firstly, the cells were washed three times with 1x PBS and then fixed by submerging the coverslip in 4% PFA for 15 minutes. PFA was removed and the cells were washed three times with 1x PBS. Cells were then covered in 0.2% Triton X-100 for 10 minutes for permeabilization. 0.2% Triton X-100 was removed, and the cells were washed three times with 1x PBS before being blocked with 1% BSA for 10 minutes.

After the 1% BSA was removed and the cells washed again, three times with 1x PBS, the cells were incubated with 20 µL of primary antibody (mouse anti-NP antibody) for one hour. Following this, the cells were washed three times with 1x PBS and incubated, now with 20 µL of secondary antibody (mouse Alexa 488), also for one hour. After being washed three times with 1x PBS, the cells were incubated with 20 µL of DAPI to stain the cell's nucleus. During incubation with primary antibody, secondary antibody, and DAPI, the 24-well plate was covered with wet paper and protected from the light.

Lastly, the cells were washed with dH2O and were mounted in glass slides with Mowiol as a mounting medium. The glass slides were left to dry for 24h and stored at 4˚C.

3.2.6 - RNA extraction/isolation (mirVana™ miRNA Isolation Kit)

The RNA from the cell pellets obtained from the infection protocol was isolated using the Total RNA Isolation Procedure of the mirVana™ miRNA Isolation Kit. All the components in the kit were manipulated as instructed by the manufacturer.

Briefly, cells were lysed with 600 µL of Lysis/Binding Solution and then vortexed vigorously to obtain a homogenous lysate. After that, 60 µL of miRNA Homogenate Additive were added to the cells, they were then vortexed and left on ice for 10 minutes. After this, 600 µL of Acid-Phenol: Chloroform (not provided in this version of the kit) were added and mixed for 1 minute before being centrifuged for 10 minutes at 10 000 x g, at room temperature. This centrifugation served to separate the aqueous and organic phases. The centrifugation should be repeated if the aqueous and organic phases were not well separated.

With both phases separated, the aqueous phase was removed to a different 2ml eppendorf while the collected volume was noted. Subsequently, 100% ethanol was added to the aqueous phase (the amount of 100% ethanol added should be 1,25x the amount of aqueous phase removed). At this point, up to 700 µL of the aqueous phase/ethanol mix were pipetted to a collection tube with a filter cartridge. The collection tubes with the cartridges were then centrifuged for 15 seconds at 10.000 x g at room temperature, and

the flow-through was discarded. This step was repeated, in the same filter cartridge, until all the mix was centrifuged.

For the washing process, firstly, 700 µL miRNA of Wash Solution 1 was applied to the Filter Cartridge and it was then centrifuged for 10 seconds at 10 000 x g at room temperature, and the flow-through was discarded. Following this, 500 µL of Wash Solution 2/3 was applied and centrifuged just like the previous step. This last step was repeated and then, the empty collection tube and filter cartridge was centrifuged for 2 minutes to remove the residual fluid from the Filter Cartridge. The Filter Cartridge was then transferred into a fresh collection tube and MiliQ Water (not included in the kit) was applied to the center of the filter and the collection tube was centrifuged again at 10 000 x g for 30 seconds, at room temperature to collect the eluate with RNA.

The obtained RNA was then quantified using the DeNovix DS-11 spectrophotometer (Nanodrop) and then stored at -80°C.

3.2.7 - RNA quantification

The DeNovix DS-11 spectrophotometer (Nanodrop) was used to quantify the RNA obtained from the extraction with the mirVana™ miRNA isolation kit like previously mentioned. First, the "Blank" was defined using MiliQ Water from the same aliquot used for the RNA elution process in the RNA extraction protocol. After the "Blank" was established, the RNA in all samples was quantified (max absorbance at 260 nm).

3.2.8 - Northern Blot

The RNA samples obtained from the mirVana™ kit extraction protocol was run in a 10% Polyacrylamide-Urea Gel (1.5 mm).

The 10% Polyacrylamide-Urea Gel (21 g of UREA, 12.5 ml of 19:1 Polyacrilamide, 5 ml TBE 10x, and MiliQ Water up to 50 ml) allowed for the separation of RNA molecules according to their molecular weight.

The pre-run was carried out at a constant voltage of 200V for 30 minutes in TBE 1x. During this pre-run, the samples were prepared by mixing the RNA (15 µg) and MiliQ water for a total volume of 30 µL. 30 µL of Loading Buffer (provided in the mirVana™ miRNA Isolation Kit) was then added to the RNA samples.

The mix was loaded in the 10% Polyacrylamide-Urea Gel and the gel was run at a constant voltage of 275V for 90 minutes. The size of the tsRNAs was determined by comparison with a parallel running DynaMarker® Prestained Marker for Small RNA Plus weight marker.

The 10% Polyacrylamide-Urea Gel was later transferred into a Hybond™-N+ nylon membrane using a semi-dry system for 35 minutes. The RNA and membrane were bonded through UV Cross-Link with a UV Stratalinker using 1200 mJ/cm2 for 1 minute, on both sides of the nylon membrane.

The membrane was later pre-hybridized with 10 ml of a Hybridization Buffer for 2 hours before the tsRNA_GlyGCC 5'-[DY782] GA GAA TTG TAC CAC TGA ACC A [DY782]-3' or the tsRNA_GluCTC 5'-[DY 782] GC CGA ATG CTA ACC ACT AGA CCA CCA [DY782]-3' probe was added for overnight incubation. In the following day the membrane was

washed using a Washing Buffer at RT for 2-3 minutes. At last, the membrane image was acquired with the Odyssey machine.

3.2.9 - cDNA synthesis

With the Applied Biosystems™ High-Capacity RNA-to-cDNA™ kit, the RNA obtained with the mirVana™ miRNA Isolation Kit was used for cDNA synthesis. The cDNA synthesis followed the manufacturer's instructions.

Every sample reaction used 500 ng of RNA plus RNAse-free water (MiliQ Water) to make up 9 µL of total volume. 10 µL of RT Buffer Mix and 1 µL of RT Enzyme Mix (both provided in the kit) were also added to each sample for a final volume of 20 µL.

The samples were spined to get rid of any air bubbles and placed in the thermal cycler. To start the reaction, the samples were incubated at 37°C for 1 hour. The samples were then heated to 95°C for 5 minutes (to stop the reaction) and was then held at 4°C until the samples were collected. The cDNA was stored at -30°C.

3.2.10 – RT-qPCR

An RT-qPCR was run with the previously synthesized cDNA. Every sample mix consisted of 10 µL of TaqMan™ Gene Expression Master Mix and 1 µL of cDNA. 1µL of the Taqman® Gene Expression Assay we intended to test (Angiogenin and GAPDH, used as a housekeeping gene) and 8 µL of RNAse-free water (MiliQ Water) to make up a final volume of 20 µL was added to every sample mix. Each condition was replicated twice.

The final mix was vortexed and 20 µL was placed in each well of a standard 96-well reaction plate, which was covered with a sealing adhesive film quickly after. Before the reaction started, the 96-well plate was centrifuged for 1 minute at 1000 rpm to remove any air bubbles. The reaction process started with a 2-minute hold at 50° C, followed by a 10-minute hold at 95° C, to activate the polymerase. It was followed by a 40-cycle period (with each cycle consisting of 1 minute) of denaturation-annealing-extension at 60°C.

3.2.11 - Transfection of synthetic 5'-Gly-GCC tsRNA mimic and infection

On the previous day, A549 cells were plated into a 6-well plate in 2 ml of complete DMEM. On the day of the transfection, the medium was switched to DMEM supplemented with 10% FBS (without antibiotics) at least one hour before transfection was initiated.

The mimics used were a synthetic 5'-Gly-GCC tsRNA mimic (5'-GCAUGGGUGGUUCAGUGGUAGAAUUCUCGCCUG-3') and a synthetic Scramble-tsRNA mimic (5'-GUGGUAGAGGUUGCUAUCU-3'), that was used as control.

A mix of 2 µl of Lipofectamine 2000 and 2 µl of Opti-MEM (for each well) was prepared and incubated for 5 minutes at RT. The mimic solutions consisted of 48 µL of the respective mimic + 356 µL of Opti-MEM in a final concentration of 10 nM.

The Lipofectamine 2000 and Opti-MEM mix was added to the mimic solutions. The new mix was incubated for 30 minutes at 37°C, 5% CO2. After incubation, 404 µL of this

mix was added to each well, drop by drop. The plate was then shaken to promote endocytosis and then incubated at 37°C, 5% CO2 for 48 hours.

After 48h, the cells were infected with IAV PR8 (with MOI of 3). A mix of infection medium and IAV PR8 was prepared, and 1 ml of this mix was added to each well, after the medium was removed and the cells were washed with 1x PBS. One hour later, an overlay with SFM and 0,14% BSA was prepared, and 1 ml was added to each well after the medium was removed and the cells were rinsed with acid wash and washed with PBS. The 6-well plate was then incubated for 16 hours at 37°C, 5% CO2.

The cells and supernatant of each well were then collected and frozen at -80°C for further use.

3.2.12 - Plaque assay

On the previous day, MDCK cells were seeded in a 12-well plate in 1 ml of complete DMEM.

Before starting the plaque assay, the supernatants (collected at the end of the infection of transfected cells) were defrosted. A serial dilution set with dilutions from 10^{-1} to 10^{-5} was prepared. 55 µl of each supernatant were added to 500 µl of SFM, vortexed, and 55 µl of that solution was subsequently diluted.

After the dilutions were prepared, the medium from the 12-well with MDCK cells was removed and the cells were washed with PBS 1x. After this, 300 µL of the dilutions from 10^{-3} to 10^{-5} were added to the MDCK cells. The 12-well plate was left on the rocker for 10 minutes, before being incubated for approximately 40 minutes at 37°C, 5% CO2.

During incubation, a medium with 12,5 ml of 2,4% Avicel, 12,5 ml of SFM, 0,5 ml of 7% BSA, and 25 µL of 1:1000 TPCK-Trypsin was prepared. When the incubation time was over, 1 ml of this medium was added to each well and the cells were incubated again at 37ºC, 5% CO2 for 36 hours to 48 hours.

After this second incubation, the medium was removed carefully without touching the base of the well. The cells were washed twice with PBS 1x and then 500 µL of 4% PFA with 0,1% toluidine blue was added. The 12-well plates were left on the rocker overnight.

In the morning, the solution was removed from the wells and the cells were washed with tap water. The number of plaques formed was counted in the dilution with more and better plaques.

3.2.13 - Statistical analysis

The statistical analysis was made using GraphPad Prism 9.1. Northern Blot quantification was performed using Image Studio Lite Version 5.2. The data was obtained from at least three independent replicas/experiments. Graph bars represent means with standard deviation (SD). Statistical significance between the various time points and the control (mock) was determined using a parametric T-test, assuming Gaussian distribution. A P-value of $< 0,05$ was considered significant.

Chapter IV – Results

4.1 Production of tsRNAs during Influenza A virus infection

In recent years, tsRNAs have been found associated to various diseases, although it is still unknown whether these small RNAs play an active role or contribute to disease pathogenicity[55].

To determine if IAV infection induced the generation of tsRNAs, we infected A549 cells with IAV PR8 (A/Puerto Rico/8/1934 (H1N1). Cell pellets were collected for RNA isolation. To confirm infection, we analysed the intracellular localization of the viral protein NP by immunofluorescence. Cells were fixed in glass coverslips and stained with anti-NP primary antibody and DAPI (for nuclear staining). Different infection time-points were assessed, namely 2 hours post-infection (hpi), 4 hpi, 6 hpi, 8 hpi and 12 hpi. Non-infected samples (mock) were used as the control condition. NP location varies during IAV infection: at 2 hpi the viral genome is still in the cytoplasm and no NP is yet observed, at 4 hpi NP is visible inside the nucleus, at 6 hpi some NP can already be detected at the cytoplasm and after 8 hpi most NP localizes at the cytoplasm with, at 12 hpi, being also present at the cell membrane, as newly formed viral particles are ready to leave the cell.

Microscopy analysis indicated that the infection was successful, as NP signal (in green) was only found in cells infected with PR8 and its location at all the time points coincided with the expected pattern (**Figure 4**)[5,10].

RNA was isolated from infected cells and mock cells, at each of the mentioned time points, using the mirVana™ miRNA Isolation Kit. Isolated RNA was analysed in a 10% Polyacrylamide-Urea gel, where 15 µg of total RNA (for every sample) were loaded. An RNA weight marker was run alongside the samples to estimate the weight of the detected tsRNAs. The 10% Polyacrylamide-Urea gel was transferred to a nylon membrane that was then incubated with non-radioactive probes: tsRNA_GluCTC 5'-[DY 782] GC CGA ATG CTA ACC ACT AGA CCA CCA [DY782]-3' (for 5'-Glu-CTC tsRNAs) or tsRNA_GlyGCC 5'-[DY782] GA GAA TTG TAC CAC TGA ACC A [DY782]-3' (for 5'-Gly-GCC tsRNAs). At least three biological replicas were performed. The mature tRNAs and tsRNAs were quantified and normalized for mock (non-infected cells).

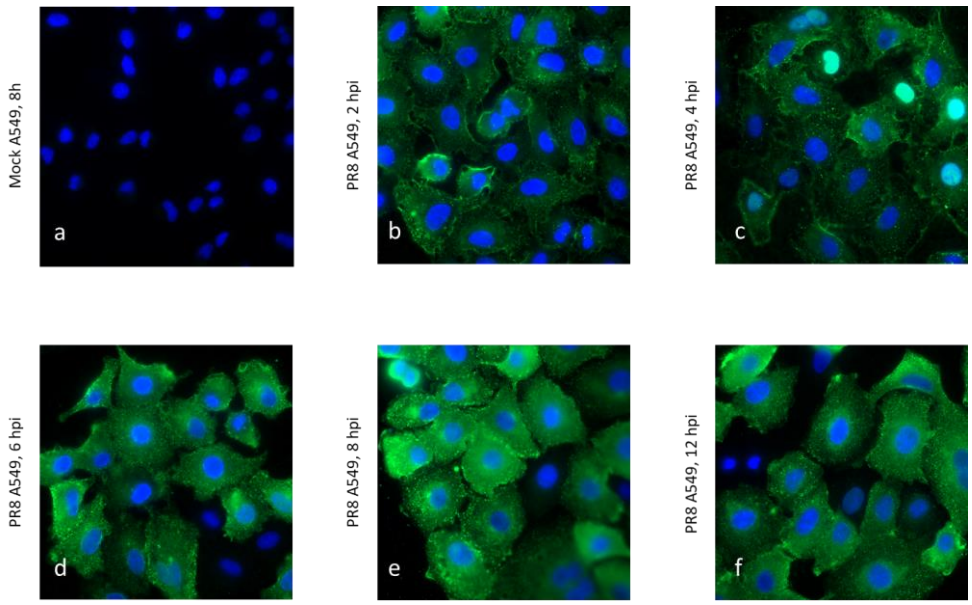

Figure 4 – Successful viral infection by IAV PR8 in A549 cells. Images by fluorescence microscopy of immunofluorescence staining of NP (anti-NP antibody) and the cell nucleus (DAPI). **a)** A549 mock-infected cells 8 hours after incubation. **b)** Infected A549 cells at 2 hpi. **c)** Infected A549 cells at 4 hpi. **d)** Infected A549 cells at 6 hpi. **e)** Infected A549 cells at 8 hpi. **f)** Infected A549 cells at 12 hpi. Viral protein NP is shown in green, and nuclei are shown in blue.

After the membrane was incubated with the tsRNA_GluCTC 5'-[DY 782] GC CGA ATG CTA ACC ACT AGA CCA CCA [DY782]-3' probe, for the detection of 5'-Glu-CTC tsRNAs, we observed two bands with a size of approximately 50 nts and 40 nts, respectively, that may represent two different tiRNAs (**Figure 5 a**), due to the fact that they are longer than 40 nts.

Quantification of the mature tRNAGlu(CTC) (**Figure 5 b**) showed no statistical difference in the quantity of mature tRNA at 2 hpi, 4 hpi, 6 hpi, 8 hpi, and 12 hpi, compared to the mock condition (non-infected cells).

The two detected tsRNAs were quantified and, in both cases, the production of these fragments was always higher during IAV infection compared to non-infected cells (**Figure 5 c** and **d**). The two fragments also shared a similar trend, where the production of both tsRNAs was higher at 2 hpi (peak production) and at 4 hpi, but decreased after that.

In the case of the tsRNA of ≈50 nts (**Figure 5 c**), statistical analysis showed statistical difference at 2hpi, 6 hpi, and 8 hpi, comparatively to mock. At 4hpi and 12 hpi, no statistical difference was detected.

On the other hand, the ≈40 nts tsRNA (**Figure 5 d**) only showed a statistical difference at 4 hpi, even though production was higher than in non-infected cells, in all the other timepoints.

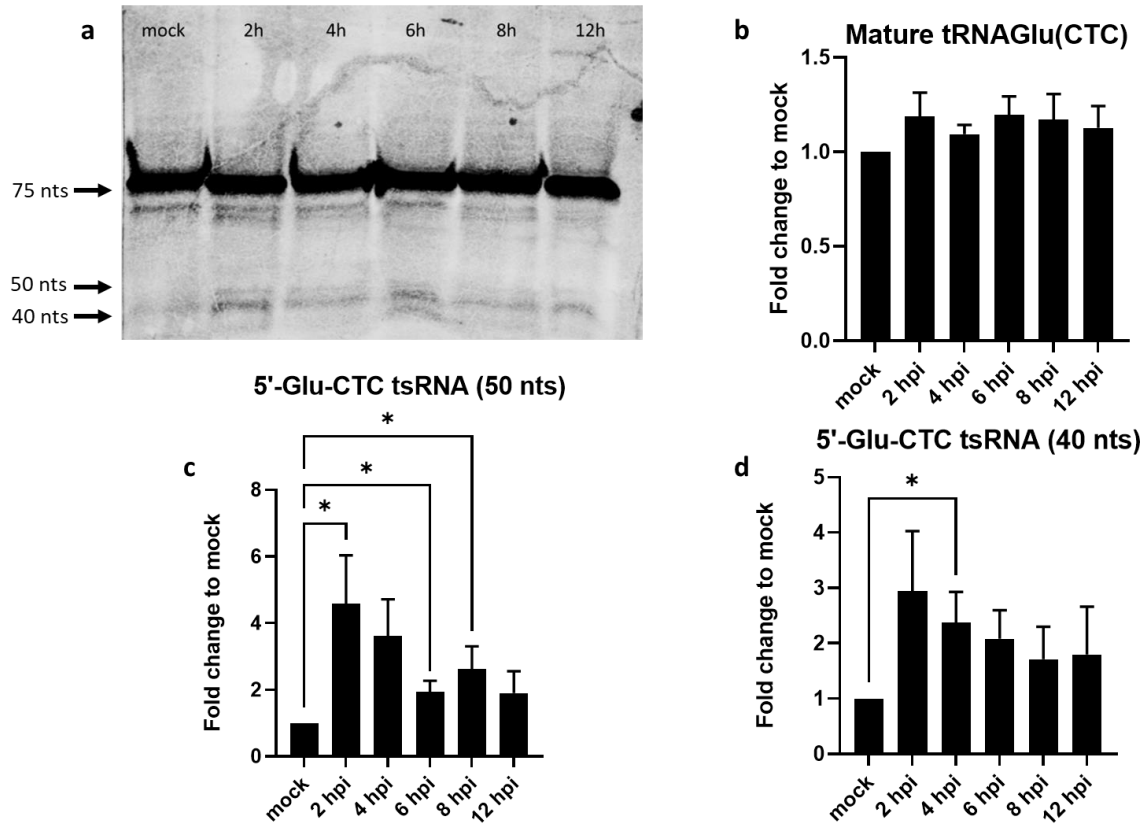

Figure 5 – Northern Blot, quantification and analysis of tRNAGlu(CTC) and 5'-Glu-CTC tsRNAs production on IAV infected A549 cells. a) Northern blot of IAV infected A549 cells, using the tsRNA_GluCTC 5'-[DY 782] GC CGA ATG CTA ACC ACT AGA CCA CCA [DY782]-3' probe to detect 5'-Glu-CTC tsRNAs and mature tRNAGlu(CTC) **b)** Quantification of mature tRNAGlu(CTC) expressed during IAV infection, at different time points. **c)** Quantification of the ≈50 nts 5'-Glu-CTC tsRNA, detected by northern blot, and analysis of its production at different timepoints comparatively to mock-infected cells. **d)** Quantification of the ≈40 nts 5'-Glu-CTC tsRNA, detected by northern blot, and analysis of its production at different timepoints comparatively to mock-infected cells. Data represent the means of four independent experiments. Statistical significance was evaluated by T-test, comparing mock-infected cells to the infected cells at different time points (2 hpi, 4 hpi, 6 hpi, 8 hpi, and 12 hpi)(*$P < 0.05$).

Incubation with the tsRNA_GlyGCC 5'-[DY782] GA GAA TTG TAC CAC TGA ACC A [DY782]-3' probe, for detection of 5'-Gly-GCC tsRNAs in PR8 infected cells, identified two tsRNAs of ≈50 nts and ≈40 nts (**Figure 6 a**)

After quantification of the mature tRNAGly(GCC) (**Figure 6 b**) we observed that there was a tiny variance, of no statistical difference, between the non-infected cells and the infected cells, in all the time points.

The production of the detected ≈50 nts 5'-Gly-GCC tsRNA (**Figure 6 c**) was higher in IAV infected cells at 4 hpi and 6 hpi, and lower at 2 hpi, 8 hpi, and 12 hpi when compared to mock-infected cells. Only at 4 hpi statistical difference was detected.

The tsRNA with ≈40 nts (**Figure 6 d**) production was higher during all observed time points compared to non-infected cells. This tsRNA was produced the most at 4 hpi and 6 hpi, where the statistical difference was detected.

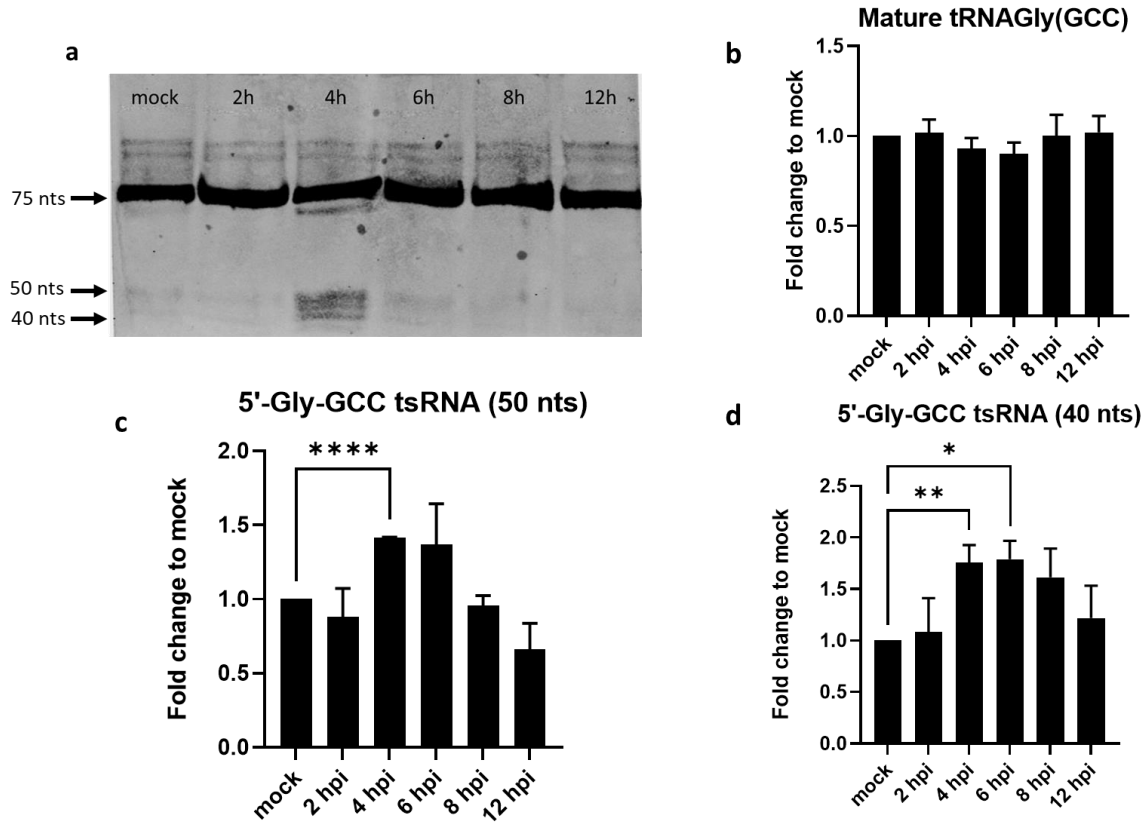

Figure 6 – Northern Blot, quantification and analysis of tRNAGly(GCC) and 5'-Gly-GCC tsRNAs production on IAV infected A549 cells. a) Northern blot of IAV infected A549 cells, using the tsRNA_GlyGCC 5'-[DY782] GA GAA TTG TAC CAC TGA ACC A [DY782]-3' probe to detect 5'-Gly-GCC tsRNAs and tRNAGly(GCC). **b)** Quantification of mature tRNAGly(GCC) expressed during IAV infection at different time points. **c)** Quantification of the ≈50 nts 5'-Gly-GCC tsRNA, detected by northern blot, and analysis of its production at different timepoints comparatively to mock-infected cells. **d)** Quantification of the ≈40 nts 5'-Gly-GCC tsRNA, detected by northern blot, and analysis of its production at different timepoints comparatively to mock-infected cells. Data represent the means of three independent experiments. Statistical significance was evaluated by T-test, comparing mock-infected cells to the infected cells at different time points (2 hpi, 4 hpi, 6 hpi, 8 hpi, and 12 hpi)(*P < 0.05).

In summary, during IAV infection, we detected four tsRNAs two of them were 5'-Glu-CTC tsRNAs and, the other two were 5'-Gly-GCC tsRNAs. In both cases, one of the tsRNAs had ≈50 nts, while the other had a size of ≈40 nts.

The production of both 5'-Glu-CTC tsRNAs was elevated during IAV infection at all time points, most noticeably at 2 hpi (where the production was at its highest) and 4 hpi. Production of both fragments decreased after 4 hpi.

The 5’-Gly-GCC tsRNA with the size of ≈50 nts was elevated at 4 hpi and 6 hpi, however, the 5’-Gly-GCC tsRNA with ≈40 nts was elevated at all time points. Interestingly, both showed statistical differences at 4 hpi, compared to non-infected cells. The 5’-Gly-GCC tsRNA with ≈40 nts also showed a statistical difference at 6 hpi.

4.2 Angiogenin expression during Influenza A virus infection

Since tsRNAs >40 nts are generally produced by tRNA cleavage near the anticodon by Angiogenin, it is possible that the accumulation of the 5’-Gly-GCC tsRNAs and 5’-Glu-CTC tsRNAs observed upon infection are accompanied by an increase in Angiogenin expression. This prompted us to analyze the expression levels of angiogenin during IAV infection to investigate if there was a correlation with 5’-Gly-GCC tsRNAs and 5’-Glu-CTC tsRNAs production. To test this, we used 500 ng (for each sample) of the previously isolated RNA for cDNA synthesis, and then, through RT-qPCR, we analyzed angiogenin expression. During RT-qPCR we used GAPDH as an endogenous control. Expression values were normalized with GAPDH.

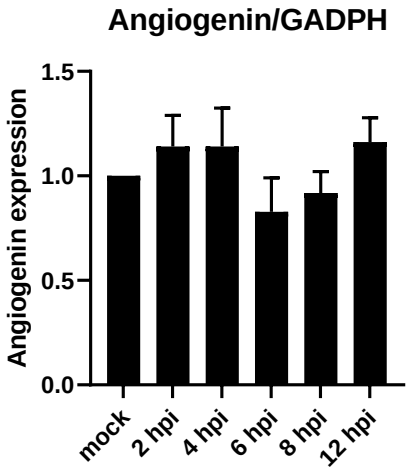

Figure 7 - RT-qPCR analysis of the expression levels of angiogenin during IAV infection. Expression values were registered at 2 hpi, 4 hpi, 6 hpi, 8 hpi, 12 hpi and were normalized with GAPDH.

RT-qPCR analysis of the expression levels of angiogenin showed that angiogenin levels were slightly higher at 2 hpi, 4 hpi, and 12 hpi, and lower at 6 hpi and 8 hpi comparatively to non-infected cells (**Figure 7**), however, none of these variations were statistically significant.

4.3 Effect of 5’-Gly-GCC tsRNAs in IAV infected A549 cells

tsRNAs have been linked to viral infection[68]. In the case of RSV, particular 5’-Glu-CTC tsRNA, could enhance RSV viral replication[56].

We increased the abundance of 5’-Gly-GCC tsRNA in A549 cells through transfection of a synthetic 5’-Gly-GCC tsRNA mimic (5’-GCAUGGGUGGUUCAGUGGUAGAAUUCUCGCCUG-3’), followed by cell infection with IAV PR8, to observe if the presence of this tsRNA would have any effect on viral infection. We used a Scramble-tsRNA mimic as control and tested the effect of the 5’-Gly-GCC tsRNA mimic through plaque assay (**Figure 8**).

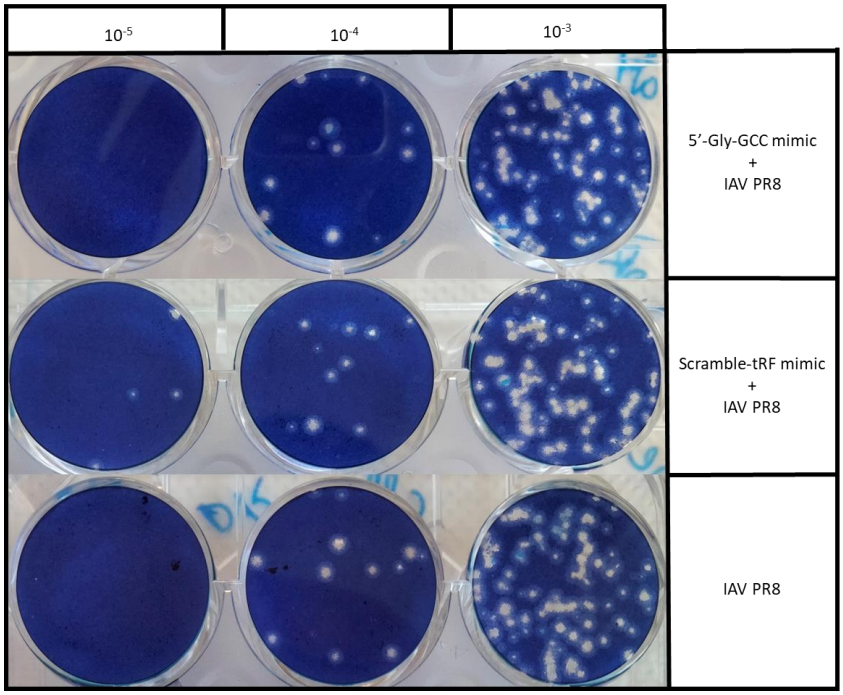

Figure 8 – Plaque assay. Supernatants used were from A549 cells transfected with 5’-Gly-GCC mimic, Scramble-tsRNA and non transfected A549 cells, infected with IAV PR8.

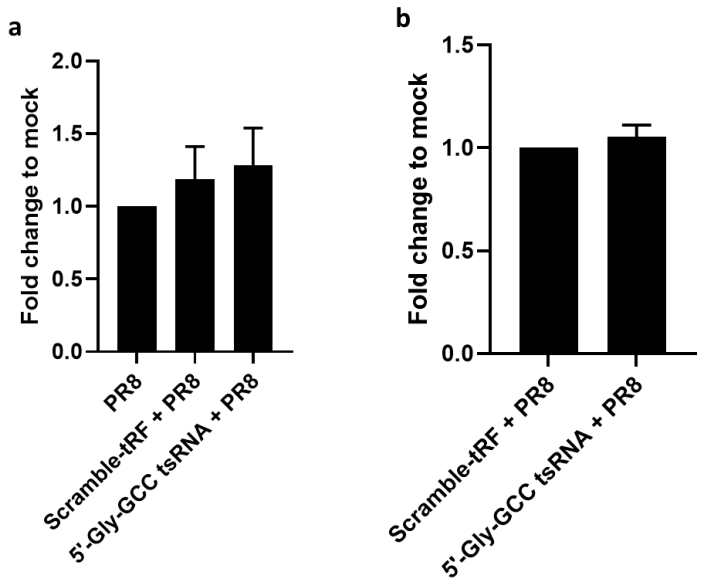

Figure 9 – Analysis of plaque formation in A549 cells transfected with 5'-Gly-GCC tsRNA mimic, Scramble-tsRNA mimic, and non-transfected cells, infected with IAV PR8. a) Analysis of the transfection process effect on plaque formation. **b)** Analysis of 5'-Gly-GCC tsRNA effect on plaque formation, comparatively to Scramble-transfected cells (control).

First, to verify if the transfection process had any effect on the cells (**Figure 9 a**), we compared IAV infected cells (PR8) with cells that were transfected with the Scramble-tsRNA mimic and 5'-Gly-GCC tsRNA mimic and later infected with PR8. We observed that cells transfected with the mimics lead to the formation of more plaques than cells that did not go through the transfection process.

We then compared the plaques formed by cells transfected with the 5'-Gly-GCC tsRNA mimic and the ones transfected with the Scramble-tsRNA mimic (**Figure 9 b**). We observed no statistical difference in the number of plaques formed in cells transfected with the 5'-Gly-GCC tsRNA mimic and the ones transfected with the Scramble-tsRNA mimic.

In summary, the higher presence of the 5'-Gly-GCC tsRNA mimic in the infected cells had no impact on IAV infection.

Chapter V – Discussion

As previously stated, the main goal of this project was to determine if IAV infection in A549 cells leads to the production of tsRNAs. tsRNAs are a novel class of sncRNAs originated by endonuclease enzymes that cleave the tRNA molecules[49]. These novel classes can be further divided into tRFs, itRFs, and tiRNAs[50]. The role of these tsRNAs is not yet understood but their potential is already recognized[56,57]. The already described presence of tsRNAs in various diseases[55] and specifically in cases of respiratory viral infections[68] led us to verify if the same would occur upon IAV infection.

Through northern blotting, using two probes, one to detect 5'-Gly-GCC tsRNAs and one to detect 5'-Glu-CTC tsRNAs, we managed to identify two 5'-Gly-GCC tsRNAs (**Figure 6 a**) and two 5'-Glu-CTC tsRNAs (**Figure 5 a**), which may represent 5'-tiRNAs, due to their size.

We first quantified the mature tRNAGlu(CTC) and the mature tRNAGly(GCC) present in our samples (**Figure 5 b** and **Figure 6 b**) and observed that the abundance of mature tRNAs was almost constant, meaning that the identified tRNA fragments were induced by specific cleavage and not just by random degradation of mature tRNAs. As it is now accepted that tsRNAs are generated through a precise biogenesis process[50] and not random by-products from the degradation of mature tRNAs as initially though[48], our results may indicate that the identified tsRNAs may have some function or role related to IAV infection. If that is the case, these tsRNAs can be potential therapeutic targets for the development of new drugs for the treatment of respiratory infections caused by IAV [54,88].

One of the 5'-Gly-GCC tsRNAs detected had a size of approximately 50 nts, while the other had a size closer to 40 nts (**Figure 6 a**). Interestingly, the two 5'-Glu-CTC tsRNAs observed also had approximately 50 nts and 40 nts, respectively (**Figure 5 a**). The size of these tsRNAs goes in line with the documented size of tsRNAs[40,49].

After quantification, we observed that the generation of the two 5'-Glu-CTC tsRNAs observed was always more abundant during IAV infection than in the non-infected cells, especially the ≈50 nts tsRNA, which presented a statistical difference at 2 hpi, 6 hpi, and 8 hpi. The ≈40 nts tsRNA only showed a statistical difference at 4 hpi (**Figure 5 c and d**).

In the case of the 5'-Gly-GCC tsRNAS, only the ≈40 nts tsRNA had a higher abundance in IAV infected cells during all time points, with statistical difference observed at 4 hpi ad 6 hpi (**Figure 6 d**). Meanwhile, the presence of the tsRNA with ≈50 was higher only at 4 hpi (the only timepoint with a significative difference) and 6 hpi and was lower at 2 hpi, 8 hpi, and 12 hpi (**Figure 6 c**).

In general, the observed tsRNAs were more prevalent at 2 hpi and 4 hpi. These time points correspond to when the viral genome enters the cell's cytoplasm (2 hpi) and enters the cell's nucleus (4 hpi), where the transcription and replication processes take place[5]. It is known that IAV doesn't innately have the necessary components to carry out these processes independently and that it hijacks the transcription machinery of the host cells[10]. The identified tsRNAs might play a role in IAV infection, namely, it is possible that these tsRNAs may have some influence over the transcription or replication processes. Previous studies found that viruses are proficient in tRNA manipulation, for example, one

of the most abundant tsRNAs in HTLV-1 infection serves as a primer by binding to the primer binding site of HTLV-1[42] and that viruses like HIV modulate the tRNA pool to improve translation efficiency[89].

Of all the types of tsRNAs, tiRNAs are the largest in size (30-50 nts) and are produced in response to stress that is characteristic of several diseases ranging from viral infection to cancer[49,68].

tsRNAs biogenesis is a precise process that involves endonuclease enzymes like Dicer, Angiogenin, and ELAC2[40,47]. These endonuclease enzymes cleave tRNAs in specific places and are usually associated with a specific type of tsRNA. For example, angiogenin is known to cleave near or at the anticodon region, being the main responsible for tiRNA formation[40,62].

Since tsRNAs > 40 nts are generally cleaved by angiogenin, we explored, through RT-qPCR, if during IAV infection the formation of tsRNAs was accompanied by an increase in angiogenin expression[40,50].

We observed that there was no significant difference in angiogenin mRNA levels at any time point, which could lead to the higher production of tsRNAs. Therefore, we concluded that angiogenin was not the endonuclease enzyme responsible for their production (**Figure 7**). However, the results of the performed replicas varied, and the CT values were high, therefore more experiments would be necessary to confirm this conclusion. Besides, protein production is not necessarily related to an increase in the mRNA levels that encodes it, since the RNA can be present but only start being translated when necessary[90]. This means that without big changes in the RNA levels, there could've been an augment in angiogenin expression. This could be assessed by western blotting, for exemple.

During RSV infection, the production of a specific 5'-Glu-CTC tRF with 31 nts is induced, and it helps promoting RSV replication[56,68]. tsRNAs, either tRFs or tiRNAs, have been linked to the facilitation of viral infection by promoting viral proliferation in RSV[56] and HIV-1[70].

As mentioned previously, the tsRNAs observed were produced mostly at 2 hpi and 4 hpi, when the virus gnome entered the cell's cytoplasm (2 hpi) and the cell's nucleus (4 hpi), where the translation and replication processes occur[5].

We transfected a synthetic 5'-Gly-GCC tsRNA mimic in A549 cells. We then infected them with IAV PR8 and performed a plaque assay to see if the high levels of this tsRNA had any effect on IAV infection.

We observed that the cells transfected with the 5'-Gly-GCC tsRNA mimic showed no difference from the control cells (transfected with a Scramble-tsRNA mimic)(**Figure 9 b**).

Chapter VI - Conclusion and Final Remarks

tsRNAs are a novel class of sncRNAs and, their role and function are only now starting to be understood. The already described presence of tsRNAs in various diseases[55] and in cases of respiratory viral infections[68] led us to verify if the same would occur upon IAV infection. Our results indicate that there is indeed the formation of tsRNAs during IAV infection. We detected two 5'-Gly-GCC tsRNAs and two 5'-Glu-CTC tsRNAs. In both cases, one had a size of approximately 40 nts while the other had a size of approximately 50 nts. In the future, the detected tsRNAs could be isolated and sequenced and, in the best-case scenario, through high-throughput sequencing technologies and microarrays, we would be able to trace the entire profile of the tsRNAs present during IAV infection and search for potential tsRNA targets. Various tsRNA studies in viral infections show that tsRNAs interact with AGO proteins such as AGO1 and AGO 4[72] and AGO 2[80], a group of proteins necessary for mammalian antiviral defenses and are also a part of the RISC complex[83]. Therefore, AGO proteins could be tested as possible tsRNA targets of the identified tsRNAs.

Our results also show that angiogenin is not the endonuclease enzyme responsible for the production of these tsRNAs. However, the results from the replicates had high variability between them, so other experimental setups such as infection of A549 cells upon silencing of angiogenin would be ideal to confirm this conclusion. A western blot for angiogenin could also help confirm or disprove our results. In the future, all the possible endonuclease enzymes potentially responsible for the formation of tsRNAs should be considered and tested.

We transfected a mimic of a 5'-Gly-GCC tsRNA into A549 cells and after that the cells were infected with IAV PR8. A plaque assay was performed to verify if the 5'-Gly-GCC tsRNA had any effect in IAV infection, namely in IAV replication, and we concluded that no visible effect was detected. However, the transfected 5'-Gly-GCC tsRNA could have caused non-visible effects that should be investigated further. In the future, it would be interesting to try the same experience with the 5'-Glu-CTC tsRNAs. Also, other avenues like testing the effect of this tsRNAs (and others if identified) in specific target-proteins.

Chapter VII – References

1. Opitz, L. *et al.* Capture of cell culture-derived influenza virus by lectins: Strain independent, but host cell dependent. *J. Virol. Methods* **154**, 61–68 (2008).
2. Matsuzaki, Y. *et al.* Clinical features of influenza C virus infection in children. *J. Infect. Dis.* **193**, 1229–1235 (2006).
3. Asha, K. & Kumar, B. Emerging Influenza D Virus Threat: What We Know so Far! *J. Clin. Med.* **8**, 192 (2019).
4. Hutchinson, E. C. Influenza Virus. *Trends Microbiol.* **26**, 809–810 (2018).
5. Dou, D., Revol, R., Östbye, H., Wang, H. & Daniels, R. Influenza A virus cell entry, replication, virion assembly and movement. *Front. Immunol.* **9**, 1–17 (2018).
6. Naulet, G., Robert, A., Dechambenoit, P., Bock, H. & Durola, F. Biology of influenza. *European J. Org. Chem.* **2018**, 619–626 (2018).
7. Krammer, F. *et al.* Influenza. *Nat. Rev. Dis. Prim.* **4**, 1–21 (2018).
8. Samji, T. Influenza A: Understanding the viral life cycle. *Yale J. Biol. Med.* **82**, 153–159 (2009).
9. Zebedee, S. L. & Lamb, R. A. Influenza A virus M2 protein: monoclonal antibody restriction of virus growth and detection of M2 in virions. *J. Virol.* **62**, 2762–2772 (1988).
10. Bouvier, N. M. & Palese, P. The biology of influenza viruses. *Vaccine* **26**, 49–53 (2008).
11. Matrosovich, M. N., Matrosovich, T. Y., Gray, T., Roberts, N. A. & Klenk, H. D. Human and avian influenza viruses target different cell types in cultures of human airway epithelium. *Proc. Natl. Acad. Sci. U. S. A.* **101**, 4620–4624 (2004).
12. Stegmann, T. Membrane fusion mechanisms: The influenza hemagglutinin paradigm and its implications for intracellular fusion. *Traffic* **1**, 598–604 (2000).
13. Pinto, L. H. & Lamb, R. A. The M2 proton channels of influenza A and B viruses. *J. Biol. Chem.* **281**, 8997–9000 (2006).
14. Cros, J. F., García-Sastre, A. & Palese, P. An unconventional NLS is critical for the nuclear import of the influenza A virus nucleoprotein and ribonucleoprotein. *Traffic* **6**, 205–213 (2005).
15. Plotch, S. J., Bouloy, M. & Krug, R. M. Transfer of 5'-terminal cap of globin mRNA to influenza viral complementary RNA during transcription in vitro. *Proc. Natl. Acad. Sci. U. S. A.* **76**, 1618–1622 (1979).
16. Hutchinson, E. C. & Fodor, E. Nuclear import of the influenza A virus transcriptional machinery. *Vaccine* **30**, 7353–7358 (2012).
17. Boulo, S., Akarsu, H., Ruigrok, R. W. H. & Baudin, F. Nuclear traffic of influenza virus proteins and ribonucleoprotein complexes. *Virus Res.* **124**, 12–21 (2007).
18. Fujii, Y., Goto, H., Watanabe, T., Yoshida, T. & Kawaoka, Y. Selective incorporation of influenza virus RNA segments into virions. *Proc. Natl. Acad. Sci. U. S. A.* **100**,

2002–2007 (2003).

19. Kreijtz, J. H. C. M., Fouchier, R. A. M. & Rimmelzwaan, G. F. Immune responses to influenza virus infection. *Virus Res.* **162**, 19–30 (2011).
20. Chen, X. *et al.* Host immune response to influenza A virus infection. *Front. Immunol.* **9**, 1–13 (2018).
21. Ren, Z. *et al.* Regulation of MAVS Expression and Signaling Function in the Antiviral Innate Immune Response. *Front. Immunol.* **11**, (2020).
22. Dixit, E. *et al.* Peroxisomes Are Signaling Platforms for Antiviral Innate Immunity. *Cell* **141**, 668–681 (2010).
23. Ho, A. W. S. *et al.* Lung CD103 + Dendritic Cells Efficiently Transport Influenza Virus to the Lymph Node and Load Viral Antigen onto MHC Class I for Presentation to CD8 T Cells . *J. Immunol.* **187**, 6011–6021 (2011).
24. Guo, Z. *et al.* NS1 protein of influenza A virus inhibits the function of intracytoplasmic pathogen sensor, RIG-I. *Am. J. Respir. Cell Mol. Biol.* **36**, 263–269 (2007).
25. Fernandez-Sesma, A. *et al.* Influenza Virus Evades Innate and Adaptive Immunity via the NS1 Protein. *J. Virol.* **80**, 6295–6304 (2006).
26. Sellers, S. A., Hagan, R. S., Hayden, F. G. & Fischer, W. A. *The hidden burden of influenza: A review of the extra-pulmonary complications of influenza infection*. *Influenza and other Respiratory Viruses* vol. 11 (2017).
27. Hussain, M., Galvin, H. D., Haw, T. Y., Nutsford, A. N. & Husain, M. Drug resistance in influenza a virus: The epidemiology and management. *Infect. Drug Resist.* **10**, 121–134 (2017).
28. Hope-Simpson, R. E. & Golubev, D. B. A new concept of the epidemic process of influenza A virus. *Epidemiol. Infect.* **99**, 5–54 (1987).
29. Rambaut, A. *et al.* The genomic and epidemiological dynamics of human influenza A virus. **453**, 615–620 (2008).
30. Taubenberger, J. K. & Morens, D. M. The pathology of influenza virus infections. *Annu. Rev. Pathol. Mech. Dis.* **3**, 499–522 (2008).
31. Worobey, M., Han, G. Z. & Rambaut, A. Genesis and pathogenesis of the 1918 pandemic H1N1 influenza a virus. *Proc. Natl. Acad. Sci. U. S. A.* **111**, 8107–8112 (2014).
32. Yu, H. *et al.* Characterization of Regional Influenza Seasonality Patterns in China and Implications for Vaccination Strategies: Spatio-Temporal Modeling of Surveillance Data. *PLoS Med.* **10**, (2013).
33. Belongia, E. A. *et al.* Repeated annual influenza vaccination and vaccine effectiveness: review of evidence. *Expert Rev. Vaccines* **16**, 723–736 (2017).
34. Demicheli, V., Jefferson, T., Ferroni, E., Rivetti, A. & Di Pietrantonj, C. Vaccines for preventing influenza in healthy adults. *Cochrane Database Syst. Rev.* **2018**, (2018).
35. Hay, A. J. & McCauley, J. W. The WHO global influenza surveillance and response system (GISRS)—A future perspective. *Influenza Other Respi. Viruses* **12**, 551–557

(2018).

36. Mckimm-Breschkin, J. L. Influenza neuraminidase inhibitors: Antiviral action and mechanisms of resistance. *Influenza Other Respi. Viruses* **7**, 25–36 (2013).
37. Palazzo, A. F. & Lee, E. S. Non-coding RNA: What is functional and what is junk? *Front. Genet.* **5**, 1–11 (2015).
38. Brosnan, C. A. & Voinnet, O. The long and the short of noncoding RNAs. *Curr. Opin. Cell Biol.* **21**, 416–425 (2009).
39. Ghildiyal, M. & Zamore, P. D. Small silencing RNAs: An expanding universe. *Nat. Rev. Genet.* **10**, 94–108 (2009).
40. Su, Z., Wilson, B., Kumar, P. & Dutta, A. Noncanonical Roles of tRNAs: TRNA Fragments and beyond. *Annu. Rev. Genet.* **54**, 47–69 (2020).
41. Acid, R. Structure of Matter. *Handb. Radiother. Phys.* 23–36 (2020) doi:10.1201/9781420012026-6.
42. Raina, M. & Ibba, M. TRNAs as regulators of biological processes. *Front. Genet.* **5**, 1–14 (2014).
43. Shi, H. & Moore, P. B. The crystal structure of yeast phenylalanine tRNA at 1.93 Å resolution: A classic structure revisited. *Rna* **6**, 1091–1105 (2000).
44. Spears, J. L., Rubio, M. A. T., Sample, P. J. & Alfonzo, J. D. tRNA Biogenesis and Processing. 99–121 (2012) doi:10.1007/978-3-642-28687-2_5.
45. Nunes, A. *et al.* Emerging Roles of tRNAs in RNA Virus Infections. *Trends Biochem. Sci.* **45**, 794–805 (2020).
46. Cech, T. R. & Steitz, J. A. The noncoding RNA revolution - Trashing old rules to forge new ones. *Cell* **157**, 77–94 (2014).
47. Cole, C. *et al.* Filtering of deep sequencing data reveals the existence of abundant Dicer-dependent small RNAs derived from tRNAs. *Rna* **15**, 2147–2160 (2009).
48. Lee, Y. S., Shibata, Y., Malhotra, A. & Dutta, A. A novel class of small RNAs: tRNA-derived RNA fragments (tRFs). *Genes Dev.* **23**, 2639–2649 (2009).
49. Emara, M. M. *et al.* Angiogenin-induced tRNA-derived stress-induced RNAs promote stress-induced stress granule assembly. *J. Biol. Chem.* **285**, 10959–10968 (2010).
50. Pereira, M. *et al.* M5 U54 tRNA hypomodification by lack of TRMT2A drives the generation of tRNA-derived small RNAs. *Int. J. Mol. Sci.* **22**, 1–19 (2021).
51. Veneziano, D. *et al.* Noncoding RNA : Current Deep Sequencing Data Analysis. 1–57 (2016) doi:10.1002/humu.23066.This.
52. Kumar, P., Anaya, J., Mudunuri, S. B. & Dutta, A. Meta-analysis of tRNA derived RNA fragments reveals that they are evolutionarily conserved and associate with AGO proteins to recognize specific RNA targets. *BMC Med.* **12**, 1–14 (2014).
53. Zeng, T. *et al.* Relationship between tRNA-derived fragments and human cancers. *Int. J. Cancer* **147**, 3007–3018 (2020).
54. Yu, X. *et al.* tRNA-derived fragments: Mechanisms underlying their regulation of

gene expression and potential applications as therapeutic targets in cancers and virus infections. *Theranostics* **11**, 461–469 (2020).

55. Anderson, P. & Ivanov, P. TRNA fragments in human health and disease. *FEBS Lett.* **588**, 4297–4304 (2014).
56. Deng, J. *et al.* Respiratory Syncytial Virus Utilizes a tRNA Fragment to Suppress Antiviral Responses Through a Novel Targeting Mechanism. *Mol. Ther.* **23**, 1622–1629 (2015).
57. Feng, W. *et al.* Identification of tRNA-derived small noncoding RNAs as potential biomarkers for prediction of recurrence in triple-negative breast cancer. *Cancer Med.* **7**, 5130–5144 (2018).
58. Mishima, E. *et al.* Conformational change in transfer RNA is an early indicator of acute cellular damage. *J. Am. Soc. Nephrol.* **25**, 2316–2326 (2014).
59. Schaffer, A. E. *et al.* CLP1 founder mutation links tRNA splicing and maturation to cerebellar development and neurodegeneration. *Cell* **157**, 651–663 (2014).
60. Hanada, T. *et al.* CLP1 links tRNA metabolism to progressive motor-neuron loss. *Nature* **495**, 474–480 (2013).
61. Chen, Y. & Shen, J. Mucosal immunity and tRNA, tRF, and tiRNA. *J. Mol. Med.* **99**, 47–56 (2021).
62. Saikia, M. *et al.* Angiogenin-Cleaved tRNA Halves Interact with Cytochrome c , Protecting Cells from Apoptosis during Osmotic Stress . *Mol. Cell. Biol.* **34**, 2450–2463 (2014).
63. Pavon-Eternod, M. *et al.* tRNA over-expression in breast cancer and functional consequences. *Nucleic Acids Res.* **37**, 7268–7280 (2009).
64. Shapiro, R. & Vallee, B. L. Site-Directed Mutagenesis of Histidine-13 and Histidine-114 of Human Angiogenin. Alanine Derivatives Inhibit Angiogenin-Induced Angiogenesis. *Biochemistry* **28**, 7401–7408 (1989).
65. Tavtigian, S. V. *et al.* A candidate prostate cancer susceptibility gene at chromosome 17p. *Nat. Genet.* **27**, 172–180 (2001).
66. Smith, R. A. *et al.* Cancer screening in the United States, 2018: A review of current American Cancer Society guidelines and current issues in cancer screening. *CA. Cancer J. Clin.* **68**, 297–316 (2018).
67. Wang, J. *et al.* Plasma tRNA Fragments Derived from 5’ Ends as Novel Diagnostic Biomarkers for Early-Stage Breast Cancer. *Mol. Ther. - Nucleic Acids* **21**, 954–964 (2020).
68. Wang, Q. *et al.* Identification and functional characterization of tRNA-derived RNA fragments (tRFs) in respiratory syncytial virus infection. *Mol. Ther.* **21**, 368–379 (2013).
69. Ruggero, K. *et al.* Small Noncoding RNAs in Cells Transformed by Human T-Cell Leukemia Virus Type 1: a Role for a tRNA Fragment as a Primer for Reverse Transcriptase. *J. Virol.* **88**, 3612–3622 (2014).
70. Yeung, M. L. *et al.* Pyrosequencing of small non-coding RNAs in HIV-1 infected cells:

Evidence for the processing of a viral-cellular double-stranded RNA hybrid. *Nucleic Acids Res.* **37**, 6575–6586 (2009).

71. Kim, H. K. *et al.* A transfer-RNA-derived small RNA regulates ribosome biogenesis. *Nature* **552**, 57–62 (2017).
72. Choi, E. J. *et al.* The importance of ago 1 and 4 in post-transcriptional gene regulatory function of TRF5-gluctc, an respiratory syncytial virus-induced tRNA-derived RNA fragment. *Int. J. Mol. Sci.* **21**, 1–11 (2020).
73. Pekarskya, Y. *et al.* Dysregulation of a family of short noncoding RNAs, tsRNAs, in human cancer. *Proc. Natl. Acad. Sci. U. S. A.* **113**, 5071–5076 (2016).
74. Goodarzi, H. *et al.* Endogenous tRNA-derived fragments suppress breast cancer progression via YBX1 displacement. *Cell* **161**, 790–802 (2015).
75. Cho, H. *et al.* Regulation of La/SSB-dependent viral gene expression by pre-tRNA 3' trailer-derived tRNA fragments. *Nucleic Acids Res.* **47**, 9888–9901 (2019).
76. Ivanov, P., Emara, M. M., Villen, J., Gygi, S. P. & Anderson, P. Angiogenin-Induced tRNA Fragments Inhibit Translation Initiation. *Mol. Cell* **43**, 613–623 (2011).
77. Boskovic, A., Yang Bing, X., Kaymak, E. & Rando, O. J. Erratum: Control of noncoding RNA production and histone levels by a 5' tRNA fragment (Genes and Development (2020) 34 (118-131) DOI: 10.1101/gad.332783.119). *Genes Dev.* **34**, 462 (2020).
78. Li, Q. *et al.* TRNA-Derived Small Non-Coding RNAs in Response to Ischemia Inhibit Angiogenesis. *Sci. Rep.* **6**, 1–10 (2016).
79. Thomas, S. P., Hoang, T. T., Ressler, V. T. & Raines, R. T. Human angiogenin is a potent cytotoxin in the absence of ribonuclease inhibitor. *Rna* **24**, 1018–1027 (2018).
80. Kim, H. K., Yeom, J. H. & Kay, M. A. Transfer RNA-Derived Small RNAs: Another Layer of Gene Regulation and Novel Targets for Disease Therapeutics. *Mol. Ther.* **28**, 2340–2357 (2020).
81. Gong, B. *et al.* Compartmentalized, functional role of angiogenin during spotted fever group rickettsia-induced endothelial barrier dysfunction: Evidence of possible mediation by host tRNA-derived small noncoding RNAs. *BMC Infect. Dis.* **13**, (2013).
82. Zhou, J. *et al.* Identification of two novel functional tRNA-derived fragments induced in response to respiratory syncytial virus infection. *J. Gen. Virol.* **98**, 1600–1610 (2017).
83. Adiliaghdam, F. *et al.* A Requirement for Argonaute 4 in Mammalian Antiviral Defense. *Cell Rep.* **30**, 1690-1701.e4 (2020).
84. Zhou, K. *et al.* A tRNA fragment, tRF5-Glu, regulates BCAR3 expression and proliferation in ovarian cancer cells. *Oncotarget* **8**, 95377–95391 (2017).
85. Zhao, C. *et al.* 5'-tRNA Halves are Dysregulated in Clear Cell Renal Cell Carcinoma. *J. Urol.* **199**, 378–383 (2018).
86. Drino, A. *et al.* Production and purification of endogenously modified tRNA-derived small RNAs. *RNA Biol.* **17**, 1104–1115 (2020).

87. Olvedy, M. *et al.* A comprehensive repertoire of tRNA-derived fragments in prostate cancer. *Oncotarget* **7**, 24766–24777 (2016).

88. Ivanov, P. Emerging Roles of tRNA-derived Fragments in Viral Infections: The Case of Respiratory Syncytial Virus. *Mol. Ther.* **23**, 1557–1558 (2015).

89. Van Weringh, A. *et al.* HIV-1 modulates the tRNA pool to improve translation efficiency. *Mol. Biol. Evol.* **28**, 1827–1834 (2011).

90. Wang, T. *et al.* Translating mRNAs strongly correlate to proteins in a multivariate manner and their translation ratios are phenotype specific. *Nucleic Acids Res.* **41**, 4743–4754 (2013).